ChemEurJ
Research Article
doi.org/10.1002/chem.202501552
Chemistry Europe
European Chemical Societies Publishing
www.chemeurj.org

Development of CPA-Catalyzed β-Selective Reductive Amination of Cardenolides for the Synthesis and Biological Evaluation of Hydrolytically Stable Analogs

Natasha Perry,[a] Shehab Eid,[b] Gerold Schmitt-Ulms,*[b] and Pavel Nagorny*[a]

This article describes the development of novel, hydrolytically stable cardiotonic steroid analogs featuring a 3β-amine moiety instead of the commonly found 3β-carbohydrates such as oleandrose. To establish the desired 3β-configuration stereoselectively, a new method based on chiral phosphoric acid-controlled diastereoselective reductive amination with Hantzsch esters was developed. This method utilizes readily available unsubstituted (S)-BINOL-based hydrogen phosphate as the catalyst, enabling the synthesis of 13 different 5β-androsterone and digitoxigenin analogs with up to 36:1 β:α diastereoselectivity. Additionally, this strategy was applied to generate two novel oleandrigenin analogs **15a** and **15g** in 3 steps from readily available gitoxigenin. The synthetic analogs were subjected to the NCI-60 human tumor cell lines screen, and several different digitoxigenin derivatives with tumor cell growth inhibitory power in submicromolar range were identified. The subsequent in vitro evaluation of digitoxigenin and oleandrin derivatives **13a**, **13g**, **15a**, and **15g** demonstrated that these four analogs reduced steady-state ATP1A1 levels in T98G cells in the 12–96 nM range. Interestingly, only the oleandrin analog **15g** lowered also steady-state levels of the cellular prion protein (PrP^C), the main therapeutic target for the treatment of prion diseases.

1. Introduction

Cardiotonic steroids are natural products of plant or animal origin with a wide range of biological activities. The plant extracts containing these compounds have been used for centuries to treat heart disease-related conditions such as edema.[1,2] This is because cardiotonic steroids act as inotropic agents that inhibit the Na^+,K^+-ATPase (NKA) pump, thereby indirectly causing an intracellular accumulation of calcium by inducing the Na^+,Ca^{2+}-exchanger (NCX) to operate in reverse mode.[3] This, in turn, may result in stronger heart muscle (myocardium) contractions, and improved function of the cardiovascular system. In addition to the treatment of heart failure and arrhythmia, recent studies suggested that cardiotonic steroids hold promise as potential therapeutics for the treatment of many other conditions, including cancer,[4] neurodegenerative diseases,[5] and viral infections.[6] In addition, several studies suggest that cardiotonic steroids and their derivatives possess antiinflammatory[6b,7] and senolytic[8] activity and may influence peripheral and central nervous systems.[9]

Plant-derived cardiotonic steroids, known as cardenolides, feature the γ-butenolide ring at the 17β-position of the steroidal ring as well as 3β-glycosylation (cf. Figure 1A). The 3β-glycosylation site is important for their biological activity, and several recent studies explored altering the 3β-glycosylation of digitoxigenin,[10] oleandrigenin,[5b,c] cannogenol,[11] strophanthidol,[7c,12] ouabagenin[7c] acovenosigenin A,[13] and digoxigenin[14] aglycones for the synthesis and biological exploration of cardenolide derivatives with enhanced biological activity. Steroid aglycones lacking glycosylation are significantly less active in comparison to their glycosylated derivatives such as α-*L*-rhamnosides.

A limitation of cardenolides such as digoxin or oleandrin is their susceptibility to undergo metabolic deglycosylation in mammalian tissue or plasma, resulting in the accumulation of the corresponding aglycones and loss of bioactivity.[15] Several groups have explored the possibility of substituting the O-glycosidic linkage with nitrogen (Figure 1B). Unlike O-glycosides, such analogs cannot be enzymatically hydrolyzed; however, they may still retain full activity of the O-glycosylated steroids. For example, Thorson and coworkers, synthesized secondary 3-alkoxyamine-substituted digitoxigenin, which was reacted with reducing sugars to form closed-ring neoglycosides.[10c] The subsequent exploration of these semisynthetic *N*-glycosides led to the identification of several analogs with significantly higher cytotoxicity and tumor specificity against cancer cells. Remarkably, 3β-*N*-glycosides were observed to exhibit higher potency

[a] *N. Perry, Prof. Dr. P. Nagorny*
Chemistry Department, University of Michigan, 930 N. University Ave., Ann Arbor, MI 48109, USA
E-mail: nagorny@umich.edu

[b] *S. Eid, Prof. Dr. G. Schmitt-Ulms*
Tanz Centre for Research in Neurodegenerative Diseases, University of Toronto, Toronto, ON M5T 0S8, Canada
E-mail: g.schmittulms@utoronto.ca

Supporting information for this article is available on the WWW under https://doi.org/10.1002/chem.202501552

© 2025 The Author(s). Chemistry – A European Journal published by Wiley-VCH GmbH. This is an open access article under the terms of the Creative Commons Attribution-NonCommercial-NoDerivs License, which permits use and distribution in any medium, provided the original work is properly cited, the use is non-commercial and no modifications or adaptations are made.

© 2025 The Author(s). Chemistry – A European Journal published by Wiley-VCH GmbH

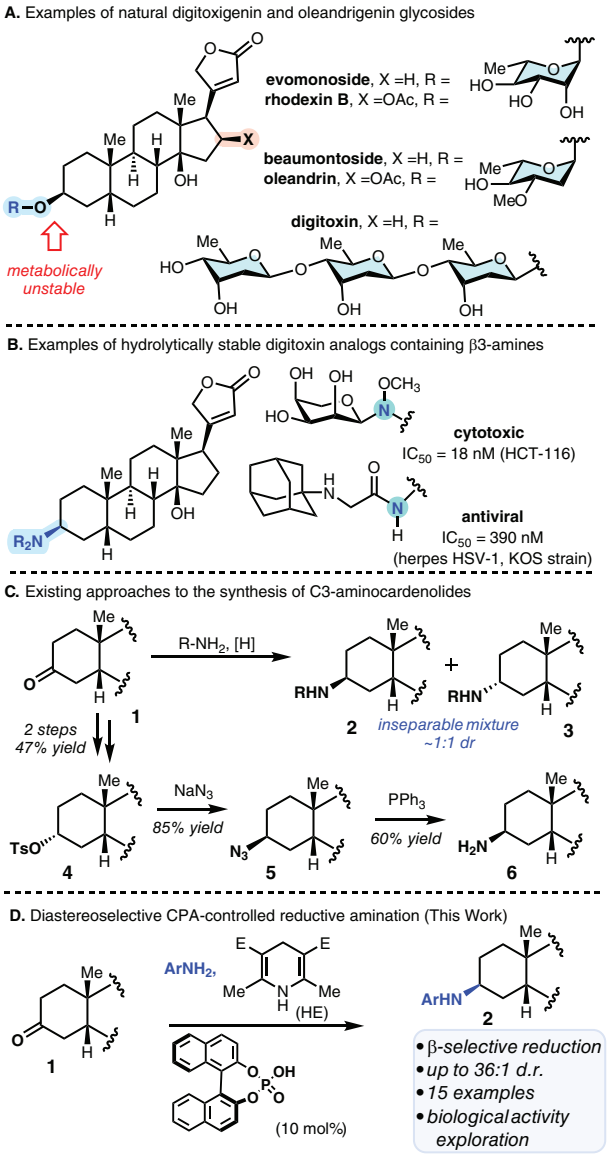


Figure 1. A) Examples of 3β-glycosides of digitoxigenin and oleandrigenin aglycones. B) Examples of bioactive digitoxin analogs with a hydrolytically stable 3β-amine moiety. C) Existing approaches for the synthesis of 3β-aminocardenolides. D) Diastereoselective CPA-controlled reductive amination developed in this work.

than their diastereomeric 3α-*N*-glycoside analogs. In related studies, various acylated 3β-amine derivatives of digitoxigenin were synthesized and their antiviral and anticancer activity was explored.[16] It was observed that such digitoxigenin derivatives possessed significantly improved activities than the unfunctionalized digitoxigenin.

While these studies highlighted the use of 3β-amine derivatives of cardiotonic steroids and demonstrated their potential for the development of more stable and bioavailable analogs, the existing methods for generating these derivatives have significant limitations. The most direct approach is based on accessing the 3-oxidized derivative **1** that could be subjected to classical reductive amination conditions (*cf.* Figure 1C).[10c,j,17] Unfortunately, such transformations lead to unselective reactions producing a ~1:1 mixture of α- and β-amines **2** and **3**, which are difficult to separate by standard flash chromatography. To avoid the aforementioned selectivity and separation problems, a different approach based on the diastereoselective synthesis of α-tosylate **4** followed by its nucleophilic substitution to generate azide **5** and its Staudinger reduction to primary amine **6** has been described.[16,18] Limitations of this 4-step protocol are that it provided **6** in only ~25% overall yield from the aglycon and that its use of azide restricts the scope of the derivatives that could be accessed through this route.

The Nagorny group has long-standing interests in developing new catalytic approaches to achieve divergent functionalization of natural products in complex settings.[7c,12,19] In addition, our recent work focused on accessing synthetic cardenolides with improved biological and pharmokinetic profiles.[5bc,7c,11,12,20] Interested in addressing the challenges associated with the synthesis of 3β-amino cardenolides, we have explored the use of chiral phosphoric acids (CPAs) as chiral catalysts that enable the diastereoselective reductive amination of the cardenolide core. This article summarizes our successful implementation of this strategy that is based on chiral phosphoric acid-controlled diastereoselective reductive amination with Hantzsch esters (HEs). This method features the use of readily available unsubstituted (*S*)-BINOL-based hydrogen phosphate as the catalyst. We showcase its versatility in the production of 13 different 5β-androsterone and digitoxigenin analogs with up to 36:1 β:α diastereoselectivity. In addition, a new concise semisynthetic route was developed to access the medicinally valuable cardenolide oleandrigenin and its 3β-aniline derivative. Finally, we assessed the potency of our synthetic analogs in a screen of 60 human tumor cell lines (NCI-60) and in an assay that monitors reductions in steady-state PrP^C levels. These efforts revealed several different digitoxigenin derivatives with tumor cell growth inhibitory power and one compound with potency for reducing PrP^C levels.

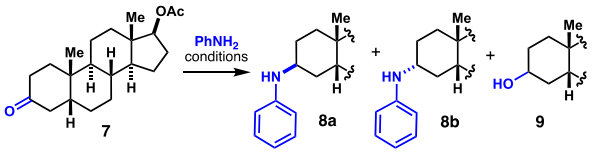
2. Results and Discussion

Although the reductive amination of 3-keto digitoxigenin with ammonia has been previously investigated (Figure 1C),[10c,j,17] this transformation was not systematically explored with other amines such as aniline. Therefore, our initial studies focused on probing the reductive amination diastereoselectivity with achiral reductants such as sodium cyanoborohydride or K-selectride® using 5β-androsterone **7** as the model system (*cf.* Table 1).[21] The exploration of sodium cyanoborohydride in different nonprotic solvents (Table 1, entries 1–3) resulted in a competitive reduction of **7** leading to **9** and minor equimolar amounts of diastereomers **8a** and **8b**. The formation of **9** was suppressed in alcoholic solvents (entries 4 and 5), and addition of 3 Å molecular sieves to methanol resulted in improved yield for **8a** and **8b** (entry 6). However, a ~1:1 mixture of diastereomers **8a** and **8b**, which are difficult to separate, was observed in all these cases.

Not surprisingly, the use of K[BH(*i*-Bu)$_3$] was not a viable option, and the formation of side-product **9** was observed in all

© 2025 The Author(s). Chemistry – A European Journal published by Wiley-VCH GmbH

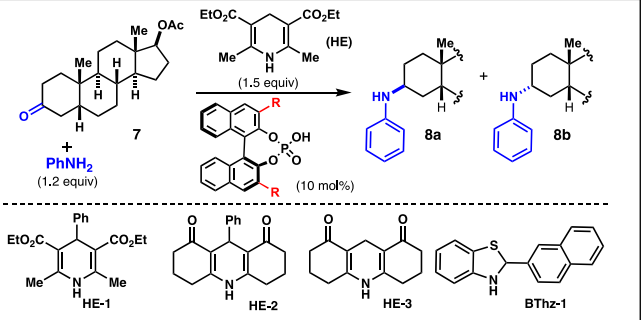
Table 1. Evaluation of hydride-based reducing agents for the 3β-selective reductive amination using model ketone **7**.[a]



Entry	Reductant	Solvent	Additive	Yield [%][b] [**8a**: **8b**: **9**]
1	$NaB(CN)H_3$	DCE	–	8:6:86
2	$NaB(CN)H_3$	DCM	–	36:25:39
3	$NaB(CN)H_3$	THF	–	11:12:78
4	$NaB(CN)H_3$	EtOH	–	29:31:0
5	$NaB(CN)H_3$	MeOH	–	36:36:0
6	$NaB(CN)H_3$	MeOH	3 Å MS	45:34:0
7	K[BH(*i*-Bu)$_3$]	MeOH/THF	Acetic acid	0:0:100
8	K[BH(*i*-Bu)$_3$]	MeOH/THF	Na_2SO_4	0:0:100
9	K[BH(*i*-Bu)$_3$]	MeOH/THF	3 Å MS	0:0:100

[a] All reactions were undertaken on a 50 mg scale using 0.1 M of the solvent described, 1.5 equivalents of $NaB(CN)H_3$ or K-Selectride®, and 1 equivalent of aniline.
[b] Isolated yields of **8a** and **8b**. DCE = dichloroethane, DCM = dichloromethane, THF = tetrahydrofuran, EtOH = ethanol, MeOH = methanol.

Table 2. Optimization of CPA-catalyzed β-selective reductive transfer hydrogenation with Hantzsch ester (HE) of model ketone **7**.[a]



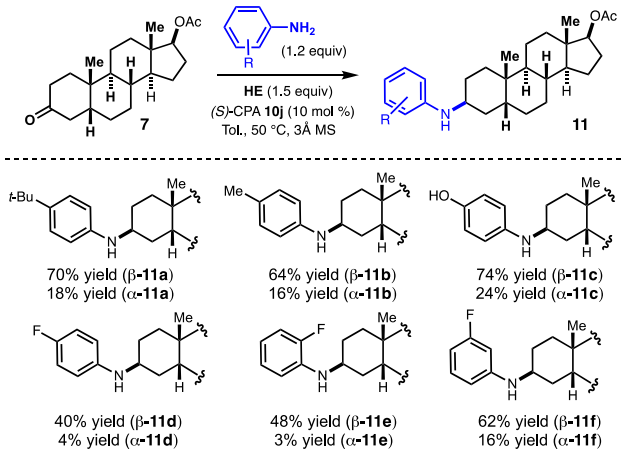
Entry	Catalyst Configuration	Catalyst 3,3′-substituent (**R**)	Solvent	Yield [%][b] [**8a**: **8b**]
1[c]	(*R*)-	3,5-$C_6H_3(CF_3)_2$ (**10a**)	MeOH	N.R.
2[c]	(*R*)-	3,5-$C_6H_3(CF_3)_2$ (**10a**)	$CHCl_3$	N.R.
3[d]	(*R*)-	3,5-$C_6H_3(CF_3)_2$ (**10a**)	PhMe	73 (57:16)
4	(*S*)-	3,5-$C_6H_3(CF_3)_2$ (**10a**)	PhMe	73 (63:10)
5	(*S*)-	3,5-$C_6H_3(SiPh_3)_2$ (**10b**)	PhMe	82 (58:24)
6	(*S*)-	2,4,6-$C_6H_2(i\text{-}Pr)_3$ (**10c**)	PhMe	54 (42:12)
7	(*S*)-	3,5-$C_6H_3F_2$ (**10d**)	PhMe	76 (60:16)
8	(*S*)-	3,5-$C_6H_3(t\text{-}Bu)_2$ (**10e**)	PhMe	56 (45:11)
9	(*S*)-	3,5-$C_6H_3Cl_2$ (**10f**)	PhMe	69 (55:14)
10	(*S*)-	3,5-$C_6H_3(SF_5)_2$ (**10g**)	PhMe	5 (4:1)
11	(*S*)-	3,5-$C_6H_3(CN)_2$ (**10h**)	PhMe	87 (74:13)
12	(*S*)-	C_6F_5 (**10i**)	PhMe	8 (7:1)
13	(*S*)-	H (**10j**)	PhMe	94 (82:12)
14[e]	(*S*)-	H (**10j**)	PhMe	N.R.
15[f]	(*S*)-	H (**10j**)	PhMe	N.R.
16[g]	(*S*)-	H (**10j**)	PhMe	35 (25:10)
17[h]	(*S*)-	H (**10j**)	PhMe	69 (63:6)

[a] Reactions in entries 1–13 were run on a 50 mg scale and reactions 14–17 were run on a 10 mg scale. All reactions were run using 0.1 M of the specified solvent, catalyst (10 mol%), Hantzsch ester (1.5 equiv), aniline (1.2 equiv), and 3 Å MS at 50 °C for 14 hours.
[b] Percent yield of **8a** and **8b** after column chromatography. The ratio of **8a**: **8b** was established by ^{1}H NMR analysis of the crude reaction mixture.
[c] These reactions were performed at room temperature.
[d] Only trace amounts of product were observed at room temperature by HRMS and TLC.
[e] The reaction was performed with **HE-1** instead of **HE**.
[f] The reaction was performed with **HE-2** instead of **HE**.
[g] The reaction was performed with **HE-3** instead of **HE**.
[h] The reaction was performed with **BThz-1** instead of **HE**. PhMe = toluene, MeOH = methanol.

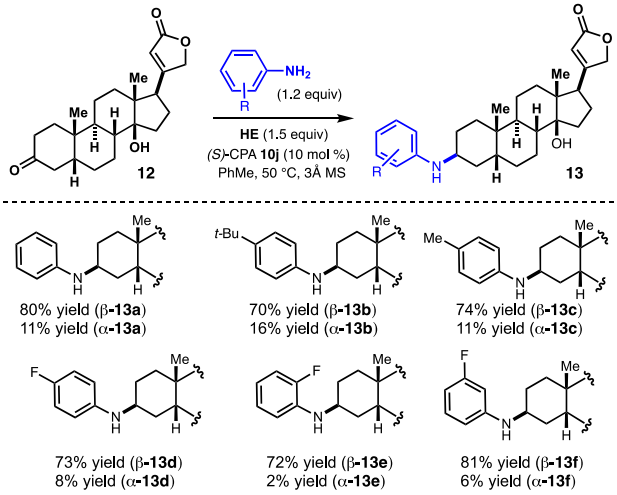
cases (entries 7–9). These results confirm the previously observed trends suggesting that reductive amination at the C3 position is unselective and leads to diastereomeric products that are difficult to separate by flash chromatography.

With these results in hand, our subsequent studies focused on exploring CPA-catalyzed transfer hydrogenation reactions with various HEs (Table 2).[22] A moderately enantioselective variant of this reaction was first attempted by Singh and Batra,[23] and then improved through CPA catalysis by the seminal work of the List, Rueping, and MacMillan groups.[24] Despite the extensive use of this transformation in the synthesis of various nitrogen-containing and heterocyclic compounds,[21b,22] to the best of our knowledge, this transformation has not been employed to achieve a diastereoselective catalyst-controlled reductive amination in the context of natural product functionalization.[25] Our initial studies began by identifying the optimal solvent and temperature conditions for the reductive amination of **7** and aniline catalyzed by 3,5-*bis*-trifluoromethylphenyl-substituted CPA **10a** (Table 2, entries 1–4).[26] Although no formation of products **8** was detected with (*R*)-CPA **10a** (10 mol%) at room temperature in methanol, chloroform, or toluene (entries 1 and 2), heating the reaction at 50 °C in toluene provided a 57:16 mixture of β:α products **8a** and **8b** in 73% yield (entry 3). The formation of the desired diastereomer **8a** was enhanced when the (*S*)- rather than (*R*)- enantiomer of **10a** was employed (entry 4). Therefore, our subsequent studies focused on evaluating various (*S*)-CPA catalysts **10b–j** (entries 5–13). We observed that the steric size of the 3,5-substituents on the phenyl ring has an impact on the selectivity of this reaction. Thus, CPAs **10d**, **10h,** and **10i** with sterically small F— and CN— 3,5-phenyl substituents promoted the highest levels of selectivity (entries 7, 11, and 12). Surprisingly, the simplest CPA **(*S*)-10j** lacking the 3,3′-aryl groups led to even higher selectivity and yield (entry 13, 94% yield, 82:12 d.r.). Finally, we attempted to enhance the selectivity by using a different hydride source in combination with **(*S*)-10j** (entries 14–17). Whereas the use of modified Hantzsch esters **HE-1** and **HE-2** did not lead to any product (entries 14 and 15), low levels of reaction conversion were noted for **HE-3** (entry 16). Remarkably, the reduction with β-naphthyl-substituted benzothiazoline (**BThz**)[27] proceeded

© 2025 The Author(s). Chemistry – A European Journal published by Wiley-VCH GmbH



Scheme 1. Exploring the scope of β-selective reductive amination of 5β-androsterone 7 with anilines[a]
[a]All reactions were run on 20 mg of **7**, with catalyst (*S*)-CPA **10j** (10 mol%), Hantzsch ester (1.5 equiv), aniline (1.2 equiv), and 3 Å MS as 0.1 M solution in toluene at 50 °C for 14 hours.



Scheme 2. Exploring the scope of β-selective reductive amination of 3-oxo digitoxigenin 12 with anilines[a]
[a]All reactions were run on 20 mg of **12**, with catalyst (*S*)-CPA **10j** (10 mol%), Hantzsch ester (1.5 equiv), aniline (1.2 equiv), and 3 Å MS as 0.1 M solution in toluene at 50 °C for 14 hours.

with excellent β-selectivity (63:6 d.r.) but was significantly slower than for the standard **HE** conditions. Therefore, the conditions used for entry 13 were selected for subsequent studies.

To evaluate the generality of the β-selective reductive amination with **(*S*)-10j** developed for aniline (*cf.* Table 2), the reaction of **7** and different substituted anilines was pursued next (Scheme 1). Similar to the reaction with aniline leading to **8a**, the reactions with alkyl-, hydroxy-, and fluoro-substituted anilines proceeded with moderate to excellent levels of β-selectivity and provided steroid derivatives **11a–11f**. It was observed that this reaction tolerates substitution at the *o*-, *m*-, and *p*-positions well. Notably, the *ortho*-fluoro derivative **11e** was obtained in 16:1 d.r., while the corresponding *meta*-substituted derivative **11f** was formed with significantly lower selectivity (~3.9:1 d.r.). Additionally, the *p*-hydroxy-substituted derivative **11c** was obtained with only a 3:1 d.r., likely due to competing hydrogen bonding interactions with the catalyst, which suppress the selective pathway.

Building on the success of the model studies with the 5β-androsterone derivative **7**, we were next prompted to explore the oxidized digitoxigenin derivative **12** (Scheme 2). This readily available compound, synthesized in one step from digitoxigenin, was subjected to the previously developed (*S*)-CPA **10j**-controlled reductive amination conditions using various anilines and **HE**, resulting in the formation of derivatives **13a–f**. Notably, despite the more complex structure and the presence of the sensitive γ-butenolide in **12**, all of these reactions proceeded with excellent yields and β-selectivities. The trends observed with 5β-androsterone derivative **7** were also seen for the derivatization of **12** albeit with higher selectivities and yields. Thus, the reaction with unsubstituted aniline provided products β-**13a** and α-**13a** in 80% and 8% yield, respectively, which aligned well with the yields obtained for **8a** and **8b** (*cf.* Table 2). Similarly, *p*-*t*-Bu and *p*-Me substituted aniline derivatives β-**13b** and β-**13c** were obtained in good yields and selectivities. Remarkably, the transfer hydrogenations with *p*-, *o*-, and *m*-fluoroanilines proceeded with significantly higher selectivities, yielding derivatives β-**13d**, β-**13e**, and β-**13f**, which were obtained in 73%, 72%, and 81% yield, respectively, with only minor amounts of the corresponding α-diastereomers.

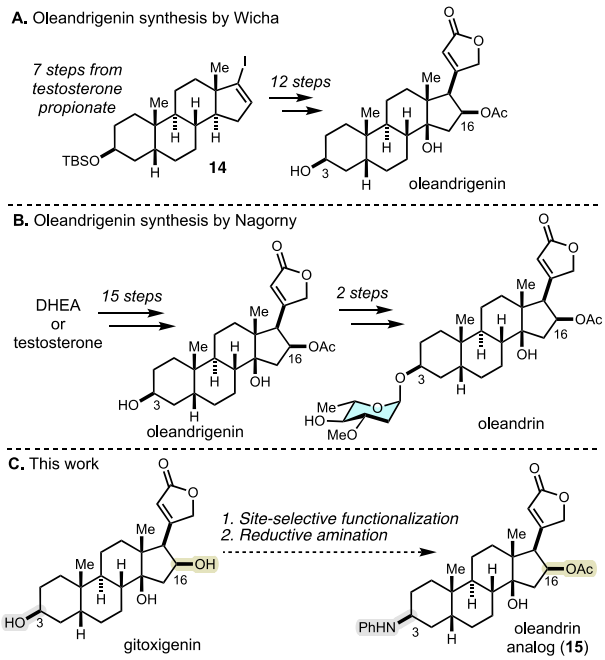


Figure 2. A) Oleandrigenin synthesis by Wicha and coworkers. B) Oleandrigenin synthesis by Nagorny and coworkers. C) Semisynthesis of oleandrin analogs from gitoxigenin presented in this work.

Our subsequent studies focused on applying this methodology to the functionalization of oleandrigenin, which is the aglycone of the natural cardenolide oleandrin found in the extracts of the Mediterranean plant *Nerium oleander* (Figure 2). Extracts containing this compound have been studied in clinical trials for the treatment of cancer and viral diseases

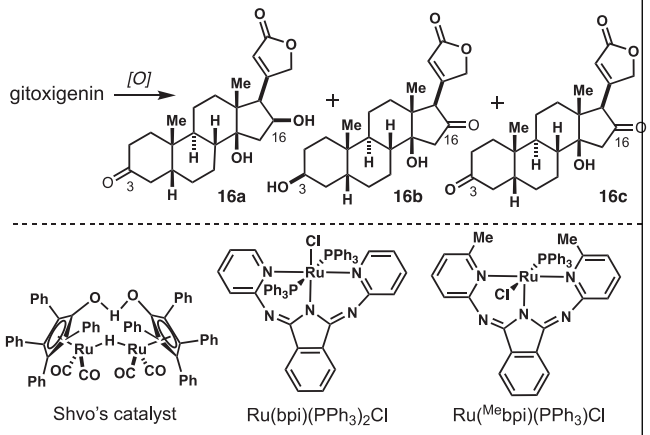
© 2025 The Author(s). Chemistry – A European Journal published by Wiley-VCH GmbH

including influenza and SARS-CoV-2.[6c,28] Recent studies suggest that oleandrin stands out amongst cardenolides in its heightened ability to cross the blood-brain barrier (BBB) and indirectly lower steady-state PrP^C levels by promoting its cointernalization and degradation alongside NKAs.[5a–c] In addition, our recent studies suggest that the brain bioavailability of oleandrin could be significantly enhanced if its sugar portion is oxidatively modified to remove the C3′ hydroxyl group.[5b] Unfortunately, SAR studies of oleandrigenin are hindered by the lower availability of this aglycone relative to the less oxidized digitoxigenin. The recent studies by the Wicha[29] and Nagorny[20b,c] groups have addressed this caveat by developing semi-syntheses protocols for oleandrigenin from testosterone and DHEA (Figure 2A,B). However, these semi-syntheses still required 15–19 linear steps and featured a late-stage photochemical singlet oxygen oxidation that limits their scale. Therefore, we focused on developing a more concise approach based on the site-selective functionalization of the more accessible gitoxigenin, the aglycone of the natural cardenolide gitoxin (*cf*. Figures 1A and 2C).

Our exploration of the site-selective functionalization of the commercially available gitoxigenin began with attempts to accomplish the selective oxidation of the 3β-alcohol to form **16a** (Table 3). Subjecting gitoxigenin to standard Dess–Martin Periodinane oxidation conditions (entry 1) indeed produced the desired C3-oxidized product **16a** (8%). Regrettably, substantial amounts of the undesired C16-oxidized regioisomeric product **16b** (80% yield), and *bis*-oxidized product **16c** (13% yield) were observed under these conditions. As the rate of TEMPO-based oxidations often correlates with the α-C-H bond dissociation energy, the combination of periodic acid and TEMPO was investigated next (entry 2).[30] Unfortunately, this protocol also favored the formation of **16b**, which was formed concomitantly with **16c**. Based on the existing precedents for the selective steroid-based polyol mono-oxidation,[31] the Corey–Kim protocol[32] was investigated next (entries 3–5), leading to an observation of extensive decomposition, which resulted in the formation of multiple products. Next, we explored the possibility of carrying out a selective C3-oxidation via transfer hydrogenation with organoruthenium catalysts (entries 6–9). The oxidation with Shvo's catalyst[33] in acetone at 55 °C proceeded with the quantitative formation of *bis*-oxidized product **16c** (entry 6). The subsequent attempts to form **16a** by oxidation with $Ru(bpi)(PPh_3)_2Cl$ or $Ru(^{Me}bpi)(PPh_3)Cl$ catalysts[34] (entries 7 and 8) or with $[Ru_2(OTf)_3(PEt_3)_6][OTf]$ (entry 9) were also unsuccessful.[35]

As an alternative to the selective C3-oxidation, we explored the possibility of producing oleandrigenin through the C16-selective acetylation of gitoxigenin (*cf*. Table 4). The acetylation with acetic anhydride in pyridine did not proceed with any observable conversion at r.t. (entry 1). Based on the encouraging precedent by the Toste, Sigman, and Miller groups,[36] the (*S*)-CPA **10j**-catalyzed reaction was explored next; however, the reaction was found to be slow, and only minor amounts of *bis*-acetylated gitoxigenin were obtained (entry 2). At the same time, addition of DMAP as the catalyst played a dramatic role on the outcome of this reaction (entries 3–4), and the desired C16-acylation product, oleandrigenin, was observed as the only regioisomer (80% yield, entry 4). The observed regioselectivity could be rationalized by higher nucleophilicity of the C16 alcohol due to its participation in intramolecular hydrogen bonding with the C14 tertiary hydroxyl group.

Table 3. Exploring site-selective oxidation of gitoxigenin.[a]



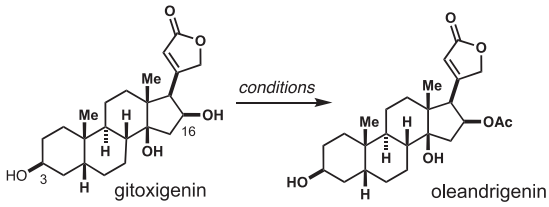
Entry	Oxidation Conditions	Outcome[b]
1	DMP (1 equiv), DCM, r.t.	**16a** (8%),**16b** (80%), **16c** (13%)
2	H_5IO_6, TEMPO, DCM, r.t.	**16b** (48%), **16c** (51%)
3	NCS, Me_2S, Et_3N	decomposition
4	NCS, $(i\text{-}Pr)_2S$, Et_3N	decomposition
5	NIS, Me_2S, Et_3N	decomposition
6[c]	Shvo's catalyst (0.6 mol%)	**16c** (99%)
7[d]	$Ru(bpi)(PPh_3)_2Cl$ (1 mol%)	decomposition
8[e]	$Ru(^{Me}bpi)(PPh_3)Cl$ (1 mol%)	decomposition
9[f]	$[Ru_2(OTf)_3(PEt_3)_6][OTf]$ (0.6 mol%)	N.R.

[a] All reactions were run on a 1 mg scale;
[b] Isolated yields of **16a**, **16b**, and **16c** are provided for entries 1, 2, and 6. The outcome of reactions in entries 3–5 and 7–9 was evaluated by ^1H NMR analysis of the crude reaction mixtures.
[c] Shvo's catalyst (0.6 mol%), acetone, 55 °C;
[d] Ru(bpi) (1 mol%), (*E*)-3,4,4-trimethylpent-2-ene (10 equiv), *t*-BuOK (10 mol%), PhMe, 110 °C;
[e] $Ru(bpi)(PPh_3)_2Cl$ or $Ru(^{Me}bpi)(PPh_3)Cl$ (1 mol%), (*E*)-3,4,4-trimethylpent-2-ene (10 equiv), *t*-BuOK (10 mol%), PhMe, 110 °C;
[f] $[Ru_2(OTf)_3(PEt_3)_6][OTf]$ (0.6 mol%), NMO, acetone, 65 °C; DMP = Dess–Martin Periodinane, TEMPO = (2,2,6,6-tetramethylpiperidin-1-yl)oxyl, NCS = *N*-chlorosuccinimide, NIS = *N*-iodosuccinimide, DCM = dichloromethane.

The direct formation of oleandrigenin from gitoxigenin enabled the evaluation of the (*S*)-CPA **10j** controlled β-selective reductive amination leading to analogs **15a–b** (*cf*. Scheme 3). Oleandrigenin oxidation with Dess–Martin Periodinane resulted in 3-oxo derivative **17** in 87% yield. We achieved the reductive amination of this compound with aniline to provide analog β-**15a** in 53% yield along with 7% of α-**15a** after column chromatography. This protocol did not lead to the cleavage of the C16-acetate moiety, a frequent obstacle to the functionalization of oleandrigenin. Subsequently, a more complex commercially available heterocyclic amine **18** was reacted with both digitoxigenone (**12**) and oleandrigenone (**17**) scaffolds to access the corresponding 3β-amines **13g** and **15g** in 45% and 52% yield, correspondingly.

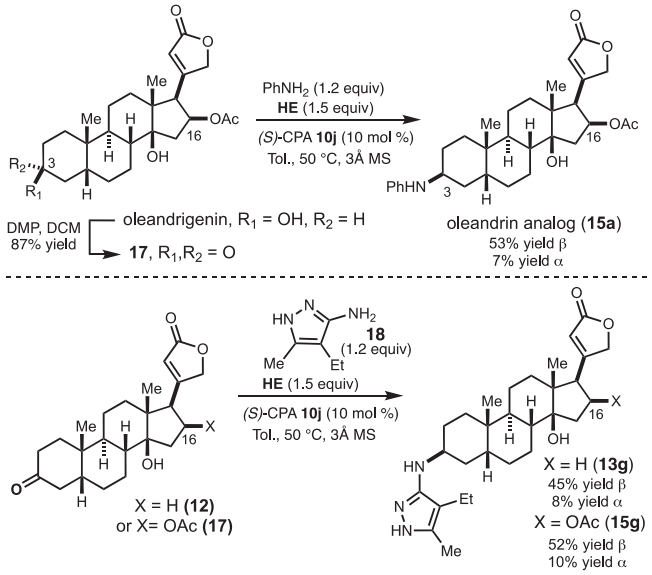
© 2025 The Author(s). Chemistry – A European Journal published by Wiley-VCH GmbH

Table 4. Site-selective acetylation of gitoxigenin.[a]



Entry	Conditions	Oleandrigenin Yield[b] [%]
1	Ac_2O (1.2 equiv), Py, r.t.	0
2	Ac_2O (1.2 equiv), (*S*)-CPA **10j** (20 mol%), PhMe (0.2 M), 4 Å MS	0 (~20% of *bis*-acetylation)
3	Ac_2O (1.0 equiv), DMAP (0.05 equiv) Py, 0 °C to r.t.	52
4	Ac_2O (1.0 equiv), DMAP (0.2 equiv) Py, 0 °C to r.t.	80

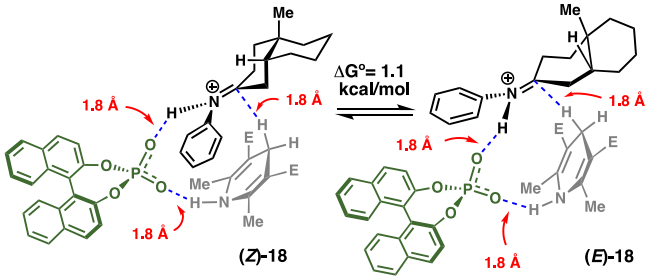
[a] Reactions in entries 1–3 were run on a 1 mg scale. The reaction in entry 4 was performed on a 18.8 mg scale.
[b] Isolated yield.



Scheme 3. Functionalization of oleandrigenin and synthesis of heterocycle-containing analogs.

Remarkably, the heterocyclic core stayed intact and did not undergo reduction under these reaction conditions.

The mechanism of the CPA-catalyzed reduction of imines with HEs has been extensively studied both computationally and experimentally, and the CPA is proposed to act as a bifunctional catalyst that brings together and activates imine and HE through the formation of two hydrogen bonds (*cf.* Scheme 4).[37] In the case of the cardenolide-derived imines leading to products **11**, **13,** and **15**, the condensation of aniline and ketone may lead to the mixture of two isomeric imines, **(*Z*)-18a** and **(*E*)-18b** that may exist in equilibrium with each other. To gain better insights into the origins of selectivity and to develop a stereochemical model, we have carried out a computational assessment of **(*Z*)-18a** and **(*E*)-18b** complexed with HE and (*S*)-CPA **10j** (Scheme 4).



Scheme 4. Computational Exploration of Stereochemical Model (DFT, B3LYP/CC-PVTZ[RCC-PVTZ], THF).

To approximate the transition states leading to the β-selective reduction of **(*Z*)-18a** and **(*E*)-18b**, the HE approached from the β-face of imine, and the distances d_1–d_3 of the broken and formed O—H/C—H bonds were constrained to 1.8 Å. The resultant complexes of **(*Z*)-18a** and **(*E*)-18b** were subjected to geometry optimization (DFT, B3LYP/6–311 + G**, vacuum) and the single point energies of the resultant structures were calculated using DFT (B3LYP/CC-PVTZ[RCC-PVTZ], THF). Based on these calculations, complex **(Z)-18** was found to be more stable by 1.1 kcal/mol. Higher stability of **(Z)-18** originates from the differences in the A-ring conformation that is required to accommodate the HE and achieve the orientation leading to the productive β-face reduction. Thus, the A-ring of **(Z)-18** was found to adopt a lower energy half-chair conformation, while the A-ring of **(*E*)-18** had to adopt a higher energy twist-boat geometry.

The successful development of the method above allowed us the synthesized analogs **8a**, **11a, 11c**, and **13a–f** in an NCI-60 human tumor cell lines screen.[38] Whereas the derivatives **8a** and **11a** did not display sufficient activity at the 10 μM concentrations, derivatives **11c** and **13a–f** were advanced to the five-dose screen (10^{-4}–10^{-8} M), and the growth inhibition 50 (GI_{50}), total growth inhibition (TGI), and lethal concentration 50 (LC_{50}) values were determined (*cf.* Figure 3). Although analog **11c** lacks the key β17-butenolide group, it exhibited moderate activity across all cancer cell lines tested. The GI_{50} values of **11c** were found to be in the range of 0.9–17.2 μM, TGI values were between 2.13–30.8 μM, and LC_{50} values were in the 4.69–55.3 μM range. In all cases, these values were found to be inferior in direct comparison to digitoxigenin (NSC# 407 806, *cf.* Figure 3).

The butenolide-containing analog **13b** functionalized with *p-tert*-butyl-substituted aniline exhibited a similar profile; however, compounds **13a**, and **13c–f** were more cytotoxic than **11c**. Compared to previously obtained NCI-60 data for digitoxigenin, **13a** and **13c–f** exhibited unique activity profiles. It is noteworthy that digitoxigenin is significantly more cytostatic,[38] than analogs **13a**, **13c–f**. With the exception of the NCI-H226 cell line (GI_{50} = 1.27 μM), digitoxigenin displayed GI_{50} values ranging in the 10–800 nM range. In contrast, the GI_{50} values for the most potent analog **13a** were observed in the 100 nM – 2.5 μM range. However, the analogs **13a**, **13c–f** displayed significant levels of cytotoxicity (LC_{50} values) for several tumor cell lines. Remarkably, in some instances, the cytotoxicity of the aniline derivatives significantly surpassed the cytoxicity of digitoxigenin. For example, these analogs had significantly higher activity against leukemia

© 2025 The Author(s). Chemistry – A European Journal published by Wiley-VCH GmbH

Cancer Cell Line	digitoxigenin			11c			13a			13b			13c			13d			13e			13f		
	GI_{50} (μM)	TGI (μM)	LC_{50} (μM)	GI_{50} (μM)	TGI (μM)	LC_{50} (μM)	GI_{50} (μM)	TGI (μM)	LC_{50} (μM)	GI_{50} (μM)	TGI (μM)	LC_{50} (μM)	GI_{50} (μM)	TGI (μM)	LC_{50} (μM)	GI_{50} (μM)	TGI (μM)	LC_{50} (μM)	GI_{50} (μM)	TGI (μM)	LC_{50} (μM)	GI_{50} (μM)	TGI (μM)	LC_{50} (μM)
Leukemia																								
CCRF-CEM	0.0297	44.4	100	1.01	2.19	4.75	0.372	1.04	3.33	1.76	3.17	5.72	1.60	2.99	5.58	0.494	1.48	3.93	0.659	1.86	4.40	0.448	1.56	4.11
HL-60(TB)	0.0524	0.298	100	1.01	2.20	4.79	0.213	0.366	0.630	2.18	3.64	6.07	2.06	3.51	5.99	0.227	0.454	0.907	1.08	2.29	4.83	0.341	1.11	3.42
K-562	0.0536	1.42	100	3.54	11.4	35.0	0.348	1.21	4.51	2.01	3.93	7.66	1.48	3.03	6.17	0.446	1.55	4.71	0.650	2.06	5.36	0.419	1.71	4.83
MOLT-4	0.0100	0.054	0.736	0.916	2.13	4.69	0.155	0.298	0.571	1.83	3.22	5.68	0.292	0.671	2.30	0.191	0.345	0.626	0.197	0.368	0.688	0.181	0.335	0.617
RPMI-8226	0.0757	0.558	100	1.56	3.02	5.84	1.19	2.70	6.15	1.80	3.25	5.88	2.31	4.41	8.44	1.42	2.91	5.94	1.69	3.29	6.40	1.45	2.90	5.81
SR	0.0531	–	100	1.61	3.01	5.63	0.210	0.400	0.761	1.71	3.09	5.56	1.20	2.45	4.98	0.245	0.566	1.75	0.532	1.69	4.12	0.319	1.04	3.23
Non-Small Cell Lung																								
A549/ATCC	0.0183	0.0455	0.135	13.2	26.2	51.9	0.267	1.26	6.66	2.73	7.77	>100	0.625	3.16	21.5	0.340	1.48	5.03	0.368	1.54	5.76	0.334	1.52	7.25
EKVX	0.0873	0.434	1.77	4.04	16.3	40.5	0.171	0.436	3.08	3.34	9.57	>100	–	–	–	0.230	0.702	4.59	0.0845	0.600	2.89	0.285	0.909	5.24
HOP-62	0.0400	0.183	0.448	–	–	–	0.272	1.05	3.28	3.00	7.30	>100	–	–	–	0.373	1.20	3.51	0.383	1.37	3.93	0.330	1.26	3.63
HOP-92	0.188	1.10	22.4	4.47	15.2	39.2	–	–	64.5	4.86	8.86	>100	>100	>100	>100	–	23.7	51.2	–	34.6	61.7	–	27.4	55.3
NCI-H226	1.27	2.82	6.27	8.76	20.9	46.0	5.74	17.8	43.8	5.83	18.5	45.2	4.07	16.1	>100	3.13	9.50	31.5	3.13	8.79	32.4	4.99	17.8	42.8
NCI-H23	0.0338	0.251	–	5.44	17.3	41.9	0.315	1.23	5.65	3.23	9.69	>100	1.35	3.37	8.45	0.380	1.42	5.89	0.637	2.35	7.65	0.449	1.84	6.79
NCI-H322M	0.169	1.18	3.19	17.1	30.8	55.7	2.07	10.9	57.2	4.97	37.3	>100	2.93	7.92	>100	2.26	14.4	68.6	2.69	9.44	>100	2.24	8.11	80.0
NCI-H460	0.0168	0.139	0.605	12.2	25.0	51.4	0.270	0.743	3.03	2.38	4.89	10.2	0.918	2.19	5.00	0.367	1.13	3.54	0.408	1.37	4.01	0.375	1.22	3.59
NCI-H522	0.0100	0.436	3.56	1.41	2.77	54.4	0.0935	0.332	1.33	2.70	5.69	19.5	0.286	0.933	–	0.188	0.490	1.93	0.209	0.532	2.32	0.177	0.462	1.72
Colon																								
COLO 205	0.440	2.32	13.3	15.7	29.3	54.6	2.22	4.44	8.89	4.75	20.1	>100	3.64	14.6	69.9	2.09	4.65	11.0	0.873	4.75	23.5	1.91	4.15	9.01
HCC-2998	0.235	0.675	2.87	15.7	29.2	54.6	–	3.67	11.5	2.26	9.77	51.0	2.50	12.0	49.5	1.56	3.91	9.80	1.71	9.06	31.0	2.32	5.76	19.3
HCT-116	0.025	0.0664	1.26	6.08	18.5	43.9	0.393	3.34	29.7	2.70	7.96	>100	1.51	4.92	>100	0.400	2.52	25.7	0.440	2.94	34.6	0.381	2.10	27.3
HCT-15	0.101	0.3	1.15	2.16	5.91	21.6	1.12	2.83	7.14	4.13	21.9	>100	3.26	9.20	>100	1.08	2.99	8.28	1.84	5.82	23.6	1.82	4.27	9.97
HT29	0.209	1.60	5.31	5.84	18.2	43.4	0.525	12.3	>100	2.53	7.11	>100	2.57	6.97	39.4	0.628	4.34	72.0	2.19	6.95	47.9	1.52	7.43	47.5
KM12	0.713	3.27	22.9	10.2	22.0	47.6	1.73	5.01	27.7	2.24	4.49	–	3.43	10.8	45.0	2.28	5.81	24.8	3.43	10.5	34.9	2.88	8.44	49.9
SW-620	0.118	1.57	22.8	14.2	27.5	53.1	0.508	7.33	37.9	3.67	11.7	47.0	2.54	7.91	32.8	0.614	3.90	25.1	0.792	10.8	35.7	0.697	6.86	40.2
CNS																								
SF-268	0.0367	0.226	1.03	14.6	27.8	53.1	0.244	–	73.8	3.76	19.7	>100	0.491	17.1	53.1	0.272	–	52.4	0.323	20.3	48.6	0.272	–	71.5
SF-295	0.0473	0.36	1.84	–	–	–	0.339	1.55	5.89	3.82	12.8	60.1	2.17	6.17	>100	0.360	1.35	3.99	0.614	3.09	14.0	0.562	2.38	7.72
SF-539	0.0356	0.160	0.453	3.27	11.5	34.2	0.218	0.984	3.32	10.7	>100	>100	0.397	1.70	4.36	0.183	1.20	3.59	0.170	1.32	3.78	0.116	1.13	3.61
SNB-19	0.85	2.20	5.26	14.4	27.6	52.9	1.18	14.7	42.9	11.0	>100	>100	3.12	8.82	96.8	1.67	10.4	38.0	0.994	7.44	29.6	2.56	10.7	45.5
SNB-75	0.299	2.12	22.8	8.24	20.3	45.3	0.302	–	34.9	3.41	14.4	>100	1.86	5.44	24.5	0.362	1.42	6.39	0.358	11.6	39.4	0.546	2.61	9.84
U251	0.199	1.52	100	–	–	–	0.763	2.16	5.33	6.13	30.4	>100	2.43	5.53	18.3	1.13	2.48	5.47	0.679	4.06	21.9	1.53	3.19	6.65
Melanoma																								
LOX IMVI	0.0547	0.533	3.84	3.58	13.3	37.1	0.503	2.12	6.53	4.89	15.0	56.2	1.99	4.93	16.6	0.691	2.12	5.19	1.34	6.77	28.1	1.10	2.74	6.83
MALME-3M	0.0615	0.522	7.69	5.81	17.9	42.5	0.547	1.36	4.01	6.53	19.2	66.6	–	–	–	0.882	2.13	4.86	0.151	0.321	0.684	1.48	2.86	5.53
M14	0.226	1.60	100	16.9	30.6	55.7	0.616	2.83	13.8	3.17	7.96	>100	1.99	3.83	7.38	0.890	2.59	7.16	0.140	0.540	2.71	1.04	2.81	7.62
MDA-MB-435	0.217	1.02	3.86	–	–	–	0.600	3.26	22.3	6.93	>100	>100	2.31	4.41	8.39	1.07	3.06	8.77	0.121	0.397	13.7	1.33	4.09	17.3
SK-MEL-2	0.321	1.56	21.3	6.30	19.2	44.2	0.570	2.38	7.83	14.6	30.8	65.1	1.99	3.99	8.01	1.12	2.70	6.52	0.625	2.49	7.88	1.37	3.03	6.71
SK-MEL-28	0.569	2.01	5.71	13.7	26.6	51.8	2.03	15.4	54.0	4.42	17.5	56.5	2.60	6.04	37.5	2.37	7.72	39.4	0.190	1.57	31.6	3.29	12.7	60.1
SK-MEL-5	0.0447	0.205	1.40	3.91	14.9	38.9	0.287	0.797	3.16	4.03	10.3	37.6	1.25	2.75	6.04	0.319	1.05	3.77	0.102	0.344	1.47	0.360	1.47	4.37
UACC-257	0.303	2.63	100	6.96	19.0	43.8	1.60	3.38	7.14	5.57	64.7	>100	–	–	>100	1.66	3.38	6.87	0.420	1.50	6.17	1.72	3.57	7.43
UACC-62	0.360	1.31	6.28	3.73	14.6	38.7	1.12	2.44	5.29	3.77	13.3	77.3	2.17	3.92	7.08	1.34	2.68	5.35	0.237	0.662	2.92	1.59	3.01	5.71
Ovarian																								
IGROV1	0.0668	2.82	100	3.74	14.8	38.9	2.15	5.82	35.3	4.73	40.4	>100	–	>100	>100	2.31	6.18	33.6	2.85	8.50	48.4	2.50	6.65	42.8
OVCAR-3	0.0367	0.204	1.94	7.89	20.6	45.7	0.361	1.44	10.2	2.63	5.80	18.3	2.02	3.80	7.17	0.512	1.90	6.83	1.27	2.96	6.87	0.702	2.33	6.66
OVCAR-4	0.0662	0.305	100	1.38	3.84	11.6	0.839	2.96	9.82	4.04	23.8	>100	–	–	>100	0.990	3.07	9.46	1.82	4.75	16.3	1.22	3.24	8.64
OVCAR-5	0.590	1.93	5.53	19.0	33.1	57.9	>100	>100	>100	11.4	54.3	>100	–	>100	>100	19.1	>100	>100	3.34	9.91	>100	>100	>100	>100
OVCAR-8	0.147	1.07	4.30	8.56	20.8	46.0	0.889	2.16	4.91	3.48	12.1	69.8	–	–	–	1.05	2.31	5.08	1.60	3.50	7.66	1.41	2.97	6.26
NCI/ADR-RES	0.115	0.573	16.6	3.12	10.2	32.5	0.521	2.04	9.35	2.22	4.37	8.60	1.95	4.10	–	0.554	2.14	7.98	1.43	3.23	7.27	0.917	3.03	9.61
SK-OV-3	0.111	0.818	5.81	17.1	30.9	55.8	0.491	2.81	31.5	4.35	27.6	>100	1.88	4.91	67.6	1.21	4.13	33.9	1.58	4.42	37.3	1.46	4.16	>100
Renal																								
786-0	0.045	0.338	0.444	6.29	19.0	43.9	0.372	1.59	10.1	–	–	–	–	–	>100	0.390	1.61	5.68	1.47	12.2	61.0	0.634	8.88	31.7
A498	0.125	0.520	100	8.07	20.5	45.7	0.384	1.37	8.30	2.88	6.81	42.5	–	–	>100	0.423	1.54	8.01	0.560	2.55	12.8	0.484	1.99	9.13
ACHN	0.0125	0.826	100	2.51	9.17	30.8	0.336	1.47	9.22	3.97	13.8	81.8	0.788	4.25	>100	0.389	1.51	7.53	0.198	1.37	–	0.377	1.78	14.6
CAKI-1	0.0357	0.180	8.04	10.5	22.5	48.1	0.379	15.0	54.6	8.30	>100	>100	2.59	7.30	92.7	0.434	11.7	51.6	0.425	2.59	>100	0.826	15.7	>100
RXF 393	0.014	0.0681	100	–	–	–	–	–	–	2.67	6.09	27.7	–	–	–	–	–	–	–	–	–	–	–	–
SN12C	0.0349	0.327	2.71	13.8	26.8	52.2	0.263	1.26	50.9	2.63	7.43	37.4	0.452	2.61	17.2	0.283	1.19	19.6	0.324	1.74	21.5	0.290	2.02	>100
TK-10	0.0944	1.59	23.9	4.71	16.7	41.1	0.304	0.805	25.1	5.07	37.9	>100	1.93	>100	>100	0.299	0.805	9.66	0.323	16.0	50.4	0.321	1.09	27.4
UO-31	0.117	4.1	100	–	–	–	0.291	0.748	2.64	6.85	33.8	>100	1.07	2.28	4.85	0.296	0.816	2.84	0.408	1.43	3.82	0.335	1.13	3.47
Prostate																								
PC-3	0.149	1.92	100	2.30	4.97	12.3	0.465	4.55	33.0	3.13	7.54	>100	1.59	4.46	21.1	0.531	3.64	28.5	0.935	3.59	17.0	0.677	4.73	38.2
DU-145	0.0400	0.146	0.411	9.51	21.4	46.7	0.291	–	>100	4.40	22.5	>100	–	>100	>100	0.377	28.6	>100	0.387	1.84	>100	0.457	36.4	>100
Breast																								
MCF7	–	–	–	6.17	19.4	44.6	0.397	2.39	21.2	4.45	29.6	>100	–	–	>100	0.568	2.64	11.8	0.548	3.96	25.1	0.634	2.91	12.7
MDA-MB-231/ATCC	0.774	62.2	100	14.8	28.0	53.2	2.81	7.01	>100	5.80	>100	>100	3.34	–	>100	2.74	6.20	99.3	2.60	6.45	24.9	2.76	6.27	>100
HS 578T	0.0673	100	100	2.69	18.0	42.7	0.172	0.561	8.36	2.57	6.75	>100	0.393	1.83	6.46	0.197	0.715	4.26	0.236	0.960	8.58	0.225	0.721	4.24
BT-549	0.0372	0.135	0.951	–	–	–	0.253	0.645	3.38	2.34	4.33	8.01	1.28	2.98	6.94	0.266	0.741	3.27	0.385	1.62	6.05	0.252	0.899	4.39
T-47D	0.292	0.859	100	2.34	8.97	30.3	2.25	5.76	>100	3.55	19.6	>100	3.23	15.6	>100	2.41	6.20	>100	2.41	6.20	>100	2.28	6.09	>100
MDA-MB-468	–	–	–	–	–	–	2.50	4.77	9.09	2.66	7.45	50.6	3.01	7.27	71.0	1.89	4.40	11.3	0.344	0.844	16.1	1.96	4.56	12.7

Figure 3. Summary of results for the NCI-60 Human Cancer Cell Line five-dose screen of compounds **11c** and **13a–f**. Each compound was evaluated against the specified cancer cell lines using five different doses (10^{-4}, 10^{-5}, 10^{-6}, 10^{-7}, and 10^{-8} M concentrations) that were normalized to control wells. The compounds **13a**, **13d**, **13e**, and **13f** were assayed twice while the five doses screen of compounds **11c**, **13b**, and **13c** was performed once. The GI_{50}/TGI/LC_{50} endpoint values provided are derived from one of the runs and are based on the linear interpolation of growth values above and below the endpoint value. The mean optical densities and the GI_{50}/TGI/LC_{50} for all experiments are provided in the Supporting Information.

cancer cells (CCR-FEM, HL-60(TB), K-562, SR) while digitoxigenin or its glycosylated analog digoxin (NSC# 7529), display relatively low cytotoxic activity (LC_{50} > 100 μM)[38] toward these cell lines. It is noteworthy that **13a** demonstrated the best overall profile against the leukemia cells with several LC_{50} values in the sub-micromolar range (0.630 μM for HL-60(TB), 0.571 μM for MOLT-4, and 0.761 μM for SR).

Our previous studies suggested that the C16-acetoxy group containing steroid oleandrin and its oxidized analog KDC203 were effective in lowering brain PrP^C levels. We documented that this capacity relied on the steroid binding to brain ATP1A1 causing endolysosomal internalization, followed by degradation of this NKA α subunit. We also showed that PrP^C, on account of residing in proximity to NKAs, gets codegraded.[5a–c] We had previously shown that this PrP^C lowering biology can be observed in several human brain cell models, including SHS-Y5Y neuroblastoma cells, ReN VM cocultures of neurons and astrocytes, and T98G gliablastoma cells. T98G cells are particularly suited for these experiments because they express PrP^C with its typical complex N-glycan modifications alongside the three NKA α subunits expressed in human brains. Therefore, our subsequent studies focused on the in vitro evaluation of oleandrin analogs **15a** and **15g** and their digitoxin equivalents **13a** and **13g** in T98 cells (Figure 4). To this end, the cells were exposed to DMSO vehicle solution or 12, 24, 48, or 96 nM solutions of compounds **13a, 13g**, **15a**, and **15g** for a duration of 6 days. Following the treatment, the cells were harvested, and cellular proteins were extracted with 0.5% NP-40, 0.5% deoxycholate, 100 mM Tris buffer (pH = 8.3), and Complete Protease inhibitor cocktail. The protein concentrations of total extracts were determined by the bicinchoninic acid (BCA) assay and adjusted, validated by consistent beta actin Western blot

© 2025 The Author(s). Chemistry – A European Journal published by Wiley-VCH GmbH

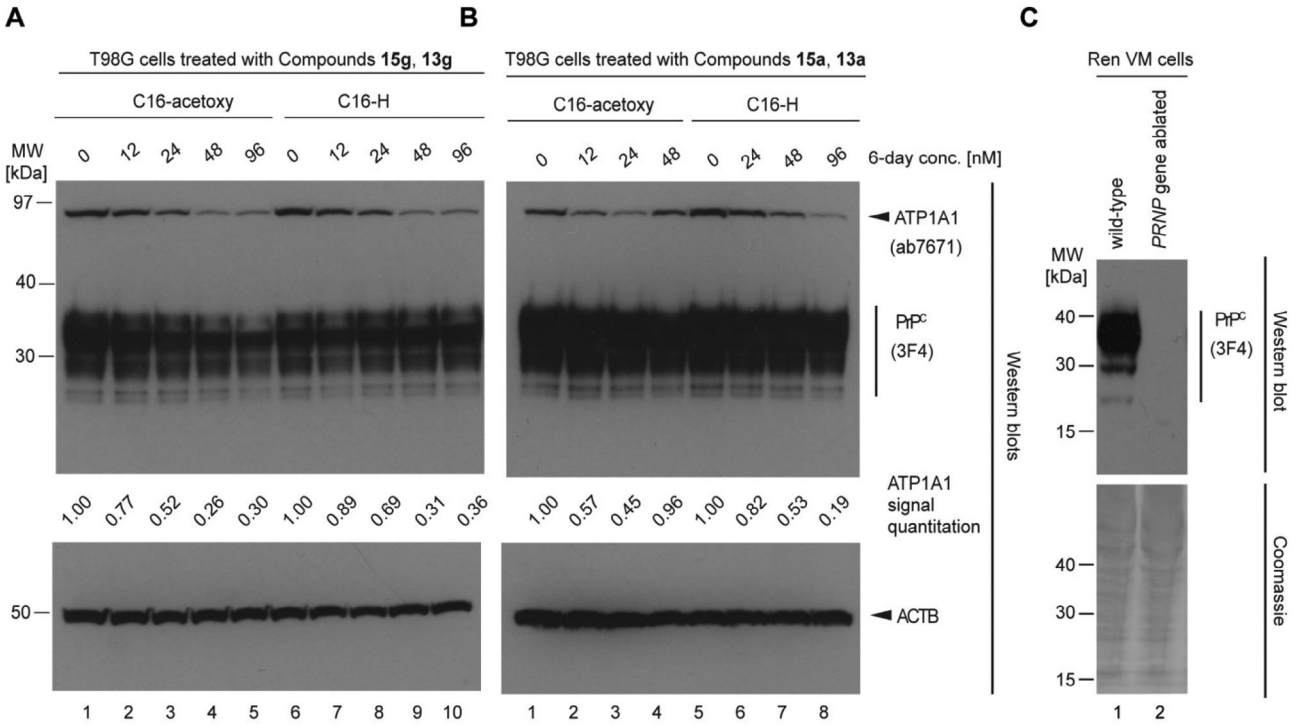


Figure 4. Western blot analysis of concentration dependent steady-state reduction of PrP levels in T98G cells. T98G cells were exposed to DMSO vehicle solution or compounds **13a, 13g**, **15a**, **15g** in DMSO at indicated concentrations for the total duration of 6 days. Following the treatment, the cells were harvested, and cellular proteins were extracted with 0.5% NP-40, 0.5% deoxycholate, 100 mM Tris/HCl buffer (pH = 8.3), and Complete Protease inhibitor cocktail. The protein concentrations were determined by bicinchoninic acid (BCA) assay and adjusted. The adjustment of total protein levels was validated by Western blot analyses of beta actin (ACTB). Western blot analysis of 20 µg of total protein per lane documented the anticipated concentration-dependent reduction of steady-state ATP1A1 for all compounds indicating target engagement. The quantitation of ATP1A1 signals was obtained by first normalizing ATP1A1 signals against signals from the ACTB loading control, followed by assigning a nominal intensity level of 1.00 to the ATP1A1 level of the mock-treated sample in each compound concentration series. A) Western Blot analysis of oleandrin analog **15g** and digitoxigenin analog **13g**. Both compounds demonstrate the reduction in ATP1A1 levels; however, only oleandrin derivative **15g** caused a concentration-dependent reduction in steady-state PrP levels. B) Western blot analysis of oleandrin analog **15a** and digitoxigenin analog **13a**. Both compounds demonstrate the reduction in ATP1A1 levels; however, no reduction in PrP^C levels was observed. Oleandrin analog **15a** was toxic at the 96 nM concentration tested, and the use of 12-well or 10-well sodium dodecyl sulfate polyacrylamide gel electrophoresis system Western blots prompted the omission of individual concentrations tested. C) Control panel documenting the exceptional specificity of the 3F4 antibody for human PrP^C, a protein giving rise to a complex band pattern due to its post-translational modification through the attachment of up to two complex N-glycan chains. The panel depicts extracts of wild-type and *PRNP*$^{-/-}$ ReN VM cells as a stand-in for T98G for this purpose because prion gene-ablated T98G cells were not available. The specificity of the ab7671 anti-ATP1A1 antibody was recently verified by us using an siRNA targeting ATP1A1 (S1 Figure, Panel B, *cf.* Ref. [39]).

signals (ACTB). Western blot analyses of 20 µg of total protein per lane documented the anticipated concentration-dependent reduction in steady-state ATP1A1 for all compounds, thereby indicating target engagement. Intriguingly, despite the consistent effect of all compounds tested on ATP1A1 levels, only the oleandrin analog **15g** mediated degradation of both ATP1A1 and PrP^C proteins. The oleandrin derivative **15a** carrying a 3β-aniline was found to be toxic at the highest concentration of 96 nM tested. Because the cells were treated with the respective compounds for a duration of six days, toxicity that impacts survival is picked up easily in this assay. Compound **15a** was not acutely deadly for the cells, but translated into slow cellular death after a few days (not shown), which restricted the subsequent Western blot analyses to a concentration range of 0–48 nM. Remarkably, the hydrolysis of the 16β-acetoxy group to the corresponding 16β-hydroxy moiety rescued the toxicity as the cells tolerated the 96 nM concentration well over the six-day assay period, but the hydrolysis also made this compound considerably less potent toward both ATP1A1 and PrP^C in this assay (*cf.* Figure Supporting Information-1).

Our prior studies suggested that the C16-acetoxy group is an important structural element that may enhance the ability of a steroid to penetrate the BBB. At the same time, the impact of the C16-acetoxy group on ATP1A1 binding was unclear, and to assess it, digitoxin analogs **13a** and **13g** lacking the C16-acetoxy group were evaluated. Both analogs demonstrated potency toward ATP1A1, with the heterocycle substituted analog **13g** exhibiting higher potency in this assay than the 3β-aniline derivative **13a**. However, both analogs were inferior to **15g** and did not induce the degradation of PrP^C. These results suggest that both the nature of the 3β-substituent and the presence of the 16β-acetoxy group are of significance for achieving cardenolide-induced reductions in PrP^C levels. Importantly, these experiments identified a new synthetic hydrolytically stable oleandrin analog (**15g**) that demonstrated promising potency toward both ATP1A1 and PrP^C.

© 2025 The Author(s). Chemistry – A European Journal published by Wiley-VCH GmbH

3. Conclusion

In conclusion, this manuscript describes a new chiral catalyst-controlled diastereoselective reductive amination of steroids featuring a *cis*-AB ring junction to generate new analogs that feature, instead of a 3β-sugar moiety, a more hydrolytically stable amine. While the traditional reductive amination methods were found to be unselective and resulted in a ~1:1 mixture of 3α- and 3β-amines that are challenging to separate, the described method capitalizes on the use of a CPA catalyst to accomplish a 3β-selective reductive amination with the HE as a hydride source. The method deploys a readily available unsubstituted (S)-BINOL-based hydrogen phosphate (*S*)-**10j** as the catalyst and was able to produce seven different 5β-androsterone analogs **8a**, **11a–f,** and six digitoxigenin analogs **13a–f** with up to 36:1 β:α diastereoselectivity. While the studies described in this work are limited to steroids containing a cardenolide core with a *cis*-AB ring junction, we anticipate that this strategy can also control the selectivity of challenging reductive aminations of other steroid or terpene-based substrates.[40] Additionally, the method generated two new oleandrigenin analogs **15a**, and **15g** in three steps from the readily available gitoxigenin. This study included the development of a site-selective C16-acetylation of the gitoxigenin triol, which was key for the subsequent generation of ketone **17** that was reductively aminated to provide **15a** and **15g** in 52% and 53% yield, correspondingly. The synthetic analogs **8a**, **11a**, **11c**, and **13a–f** were subjected to a screen of 60 human tumor cell lines (NCI-60). Analogs **11c** and **13a–f** were subsequently selected for a five-dose screen (10^{-4}–10^{-8} M) that allowed the determination of their GI_{50}, TG, and IC_{50} values for nine different cancers (leukemia, NSLC, colon, CNS, melanoma, ovarian, renal, prostate, and breast cancers, *cf*. Figure 3). All tested analogs exhibited cytostatic and cytotoxic effects against most of the tested cancer cell lines. Importantly, **11c**, and **13a–f** demonstrated significant cytotoxicity against leukemia cells, often in submicromolar range. Considering that the natural product digitoxin and its aglycone digitoxigenin exhibit low cytotoxicity (LC_{50} values > 100 μM) against most leukemia cell lines, the installation of the aniline moiety seems to be crucial to the enhanced cytotoxic activity displayed by **11c** and **13a–f**. Finally, we carried out in vitro studies with both oleandrin analogs **15a**, **15g**, and digitoxin analogs **13a** and **13g** to evaluate their potential to lower steady-state ATP1A1 and PrP^C protein levels in T98G cells. Whereas all four analogs reduced the levels of ATP1A1 in the 12–96 nM concentration range, the oleandrin analog **15g** uniquely reduced the steady-state levels of PrP^C. Although these analyses did not reveal the mechanism that distinguishes the analog **15g** from other oleandrin-derivatives in this regard, our work put a spotlight on the 16β-acetoxy group as being essential for achieving the desired PrP^C lowering effect.

4. Experimental Section

General Methods and Materials: All reactions were carried out under an atmosphere of nitrogen in flame- or oven-dried glassware with magnetic stirring. Mupirocin was purchased from Sigma Aldrich and used as such. CPAs **10a–10j** were either commercially available or could be synthesized using the known procedures. Deionized water was used in the preparation of all aqueous solutions and for all aqueous extractions. Solvents used for extraction and chromatography were ACS or HPLC grade. Purification of reactions mixtures was performed by flash chromatography using SiliCycle SiliaFlash P60 (230–400 mesh). Diastereomeric ratios were determined by ^{1}H NMR analysis. All spectra were recorded on Varian vnmrs 700 (700 MHz), Varian vnmrs 500 (500 MHz), Varian MR400 (400 MHz), Varian Inova 500 (500 MHz) spectrometers, and chemical shifts (δ) are reported in parts per million (ppm) and referenced to the ^{1}H signal of the internal tetramethylsilane according to IUPAC recommendations. Data are reported as (br = broad, s = singlet, d = doublet, t = triplet, q = quartet, qn = quintet, sext = sextet, m = multiplet; coupling constant(s) in Hz; integration). High resolution mass spectra (HRMS) were recorded on MicromassAutoSpecUltima or VG (Micromass) 70–250-S Magnetic sector mass spectrometers in the University of Michigan mass spectrometry laboratory. Infrared (IR) spectra were recorded as thin films on NaCl plates on a Perkin Elmer Spectrum BX FT-IR spectrometer and are reported in wavenumbers (cm^{-1}). The samples of pure compounds **8a**, **11a**, **11c**, and **13a–f** were submitted to the National Cancer Institute Developmental Therapeutics Program (NCI/DTP), who carried their evaluation following the standard protocols and provided the screening data of compounds present in this manuscript. Specifically, NSC# of **8a**, **11a**, **11c**, and **13a–f** are 852 083, 852 085, 852 084, 852 077, 852 082, 852 081, 852 078, 852 079, and 852 080. The results of 5-dose NCI-60 evaluation of digitoxigenin (NSC# 407 806) and digitoxin (NSC# 7529) were obtained from the National Cancer Institute website (www.dtp.cancer.gov). The mean optical densities and the GI_{50}/TGI/LC_{50} for the NCI60 screen of compounds **8a**, **11a**, **11c**, and **13a–f** are provided in the Supporting Information.

Experimental Procedures and Characterization:

Reductive amination of **7** leading to **8a**: To a flame-dried 2-dram vial with a stir bar was added the starting steroid **7** (1.0 equiv, 50.0 mg, 0.15 mmol), aniline (1.2 equiv, 16.9 μL, 0.185 mmol), the HE (1.5 equiv, 57.1 mg, 0.23 mmol), the CPA catalyst (*S*)-**10j** (5.2 mg, 0.015 mmol, 10 mol%), and the 3 Å molecular sieves. This was flushed thoroughly with nitrogen before toluene (1.50 mL) was added. The reaction mixture was placed in a preheated aluminum block at 50 °C and allowed to stir overnight under a nitrogen balloon. Once complete, the reaction mixture was filtered through cotton to remove the molecular sieves and purified by flash column chromatography. ^{1}H NMR (700 MHz, Chloroform-d) δ 7.16 (t, J = 7.7 Hz, 2H), 6.66 (t, J = 7.3 Hz, 1H), 6.59 (d, J = 7.9 Hz, 2H), 4.61 (t, J = 8.6 Hz, 1H), 3.92 (s, 1H), 3.75 (s, 1H), 2.17 (ddd, J = 15.3, 12.1, 7.4 Hz, 1H), 2.05 (s, 4H), 1.89 (td, J = 13.8, 6.9 Hz, 1H), 1.75 (d, J = 12.2 Hz, 1H), 1.60 (dq, J = 23.7, 14.1, 11.6 Hz, 5H), 1.53 – 1.39 (m, 6H), 1.33 – 1.02 (m, 7H), 0.99 (s, 3H), 0.79 (s, 3H). ^{13}C NMR (176 MHz, Chloroform-d) δ 171.4, 147.5, 129.4, 116.7, 113.0, 83.0, 51.0, 47.9, 42.9, 40.1, 37.6, 37.3, 35.6, 35.3, 31.1, 30.7, 27.7, 26.8, 26.0, 24.6, 24.2, 23.7, 21.3, 20.7, 12.2. HRMS (ESI-TOF) (*m/z*): [M + H]+ calcd for $C_{27}H_{40}NO_2$ + 410.3054, found 410.3054. IR (thin film, cm^{-1}): 3384, 2920, 2856, 2162, 1722, 1602, 1500, 1444, 1371, 1316, 1284, 1246, 1178, 1152, 1044, 1027, 986, 954, 912, 868, 834, 749, 694, 671, 607, 593, 571, 560, 551, 544, 530. $[\alpha]_D^{23}$ = +50.2 (c = 0.8, CH_2Cl_2).

Reductive amination of **12** leading to **13a**: To a flame-dried 2-dram vial with a stir bar was added the digitoxigenin derivative **12** (20.0 mg, 0.054 mmol), aniline (1.2 equiv, 5.9 μL, 0.064 mmol), the HE (1.5 equiv, 20.4 mg, 0.081 mmol), the CPA catalyst (1.9 mg, 5.5 μmol, 10 mol%), and the 3 Å molecular sieves. This was flushed thoroughly with nitrogen before toluene (0.60 mL) was added. The reaction

© 2025 The Author(s). Chemistry – A European Journal published by Wiley-VCH GmbH

mixture was placed in a preheated aluminum block at 50 °C and allowed to stir overnight under a nitrogen balloon. Once complete, the reaction mixture was filtered through cotton to remove the molecular sieves and purified by flash column chromatography. ^{1}H NMR (700 MHz, Chloroform-d) δ 7.20 – 7.12 (m, 2H), 6.66 (t, J = 7.3 Hz, 1H), 6.62 – 6.55 (m, 2H), 5.88 (d, J = 1.9 Hz, 1H), 5.00 (dd, J = 18.2, 1.8 Hz, 1H), 4.81 (dd, J = 18.0, 1.8 Hz, 1H), 3.92 (s, 1H), 3.75 (q, J = 3.1 Hz, 1H), 2.79 (dd, J = 9.1, 5.6 Hz, 1H), 2.22 – 2.10 (m, 2H), 2.06 – 1.93 (m, 1H), 1.93 – 1.80 (m, 2H), 1.77 – 1.66 (m, 3H), 1.65 – 1.37 (m, 8H), 1.34 – 1.17 (m, 6H), 0.97 (s, 3H), 0.88 (s, 3H). ^{13}C NMR (176 MHz, Chloroform-d) δ 174.7, 147.4, 129.4, 117.8, 116.9, 113.0, 85.7, 73.6, 51.0, 49.7, 47.8, 41.9, 40.1, 37.0, 35.8, 35.5, 33.3, 30.8, 30.5, 27.0, 26.8, 24.7, 24.0, 21.5, 21.3, 15.9. HRMS (ESI-TOF) (*m/z*): [M + H]+ calcd for $C_{29}H_{40}NO_3$ + 450.3003, found 450.3001; [M + Na]+ calcd for $C_{29}H_{39}NaNO_3$ + 472.2822, found 472.2816. IR (thin film, cm^{-1}): 3403, 2919, 2858, 2246, 1723, 1618, 1519, 1447, 1372, 1360, 1315, 1282, 1248, 1180, 1148, 1104, 1043, 1028, 988, 952, 909, 807, 727, 684, 646, 611, 593, 568, 551, 545, 530. $[\alpha]_D^{23}$ = +24.6 (c = 0.3, CH_2Cl_2).

Selective acetylation of gitoxigenin leading to oleandrigenin: The commercially available starting material (1.0 equiv, 18.8 mg, 0.048 mmol) was added to a flame-dried v-shaped vial and stir bar and flushed with nitrogen. Freshly distilled acetic anhydride (1.0 eq, 4.6 µL, 0.048 mmol) in 0.5 mL of pyridine and DMAP (0.20 eq, 1.2 mg, 0.096 mmol) in 0.25 mL of pyridine were added. The reaction was allowed to stir at room temperature for 14 hours. Subsequently, the solvent was removed via rotary evaporation. The white solid was redissolved in ethyl acetate and extracted with sodium bicarbonate (aq., sat., 3x) and brine (aq., sat., 1x). The organic layers were combined, dried with sodium sulfate, filtered, and concentrated by rotary evaporation. Column chromatography (20% acetone/hexane to 30% acetone/hexane) led to a white solid (80% yield, 86% BRSM). ^{1}H NMR (500 MHz, Chloroform-*d*) δ 5.97 (s, 1H), 5.47 (td, *J* = 9.3, 2.7 Hz, 1H), 5.04 – 4.93 (m, 1H), 4.86 (d, *J* = 18.1 Hz, 1H), 4.14 (t, *J* = 3.0 Hz, 1H), 3.19 (d, *J* = 8.7 Hz, 1H), 2.73 (dd, *J* = 15.7, 9.8 Hz, 1H), 1.97 (s, 3H), 1.93 – 1.83 (m, 2H), 1.81 – 1.68 (m, 3H), 1.60 – 1.40 (m, 7H), 1.39 – 1.13 (m, 7H), 0.94 (d, *J* = 7.3 Hz, 6H). ^{13}C NMR (126 MHz, Chloroform-*d*) δ 172.9, 169.6, 166.7, 121.9, 83.3, 75.1, 73.6, 66.1, 62.2, 55.9, 49.4, 41.5, 40.5, 38.6, 35.8, 35.2, 34.5, 33.4, 31.9, 29.9, 29.6, 29.4, 27.9, 26.4, 23.6, 22.7, 20.8, 20.5, 20.1, 15.5, 14.0. HRMS (ESI-TOF) (*m/z*): [M + H]+ calcd for $C_{25}H_{37}O_6^+$ 433.2585, found 433.2584. $[\alpha]_D^{23}$ = −15.4 (c = 0.2, CH_2Cl_2).

Oxidation of oleandrigenin to **17**: The starting material (29.9 mg, 0.069 mmol) was placed in a flame-dried round bottom flask with a stir bar under nitrogen. The DMP (3 equiv, 88.0 mg, 0.21 mmol) was added and then the solids were dissolved in DCM (0.70 mL). The reaction was stirred overnight at r.t. Once complete by TLC, the reaction was quenched with $NaHCO_3$ (sat., aq.) then $Na_2S_2O_3$ (sat., aq.). The reaction mixture transitioned from white to clear after 30 minutes. Then extract with DCM (3x), dry with Na_2SO_4, filter, and concentrate by rotary evaporation. The crude material was purified by flash column chromatography (SiO_2, 20% acetone/hex) to give 26.0 mg (87% yield) of the white solid desired steroid. ^{1}H NMR (500 MHz, Chloroform-*d*) δ 5.99 (t, *J* = 1.8 Hz, 1H), 5.48 (td, *J* = 9.0, 2.5 Hz, 1H), 4.97 (dd, *J* = 18.1, 1.9 Hz, 1H), 4.85 (dd, *J* = 18.0, 1.8 Hz, 1H), 3.20 (d, *J* = 8.6 Hz, 1H), 2.74 (dd, *J* = 15.6, 9.6 Hz, 1H), 2.60 (dd, *J* = 15.3, 13.6 Hz, 1H), 2.34 (td, *J* = 14.6, 5.5 Hz, 1H), 2.25 – 2.18 (m, 1H), 2.05 (dddd, *J* = 17.6, 14.4, 5.1, 2.7 Hz, 2H), 1.97 (s, 3H), 1.93 – 1.80 (m, 4H), 1.72 (td, *J* = 11.5, 3.7 Hz, 1H), 1.67 – 1.53 (m, 4H), 1.54 – 1.42 (m, 2H), 1.37 (tdd, *J* = 16.0, 13.8, 12.1, 5.6 Hz, 2H), 1.32 – 1.18 (m, 1H), 1.02 (s, 3H), 0.97 (s, 3H). ^{13}C NMR (126 MHz, Chloroform-*d*) δ 212.2, 174.1, 170.5, 167.4, 121.7, 84.2, 75.7, 73.9, 56.1, 50.1, 43.6, 42.2, 41.7, 41.3, 39.2, 37.2, 36.7, 35.2, 29.9, 26.5, 22.7, 21.2, 21.0, 20.8, 16.1. HRMS (ESI-TOF) (*m/z*): [M + H]+ calcd for $C_{25}H_{35}O_6^+$ 431.2428, found 431.2437. $[\alpha]_D^{23}$ = −13.4 (c = 0.2, CH_2Cl_2).

Reductive amination of **17** Leading to **15**: To a flame-dried 2-dram vial with a stir bar was added oleandrigenin derivative **17** (10.0 mg, 0.023 mmol), aniline (1.2 equiv, 2.5 µL, 0.028 mmol), the HE (1.5 equiv, 8.8 mg, 0.035 mmol), the CPA catalyst (0.8 mg, 0.0023 mmol, 10 mol%), and the 3 Å molecular sieves. This was flushed thoroughly with nitrogen before toluene (0.50 mL) was added. The reaction mixture was placed in a preheated aluminum block at 50 °C and allowed to stir overnight under a nitrogen balloon. Once complete, the reaction mixture was filtered through cotton to remove the molecular sieves and purified by flash column chromatography. ^{1}H NMR (700 MHz, Chloroform-*d*) δ 7.17 (t, *J* = 7.7 Hz, 2H), 6.67 (t, *J* = 7.3 Hz, 1H), 6.59 (d, *J* = 7.9 Hz, 2H), 5.98 (s, 1H), 5.54 – 5.45 (m, 1H), 4.99 (d, *J* = 18.1 Hz, 1H), 4.86 (d, *J* = 18.1 Hz, 1H), 3.76 (s, 1H), 3.20 (d, *J* = 8.7 Hz, 1H), 2.78 (dd, *J* = 15.7, 9.6 Hz, 1H), 1.98 (s, 3H), 1.97 – 1.93 (m, 1H), 1.88 (td, *J* = 13.8, 6.7 Hz, 1H), 1.80 (dd, *J* = 15.7, 2.6 Hz, 1H), 1.75 – 1.69 (m, 1H), 1.67 (td, *J* = 12.0, 3.4 Hz, 2H), 1.64 – 1.59 (m, 2H), 1.58 – 1.53 (m, 3H), 1.49 – 1.43 (m, 3H), 1.34 (td, *J* = 13.6, 3.5 Hz, 2H), 1.29 (d, *J* = 3.9 Hz, 2H), 1.23 (d, *J* = 12.9 Hz, 1H), 0.97 (s, 3H), 0.94 (s, 3H), 0.88 (t, *J* = 7.1 Hz, 1H). ^{13}C NMR (176 MHz, Chloroform-*d*) δ 174.2, 170.6, 167.8, 147.3, 129.5, 121.6, 117.0, 113.1, 84.4, 75.8, 74.0, 56.2, 50.1, 47.8, 41.9, 41.4, 39.4, 37.0, 35.8, 35.4, 30.7, 30.5, 29.8, 26.6, 24.7, 24.0, 21.2, 21.2, 20.9, 16.1, 14.3. HRMS (ESI-TOF) (*m/z*): [M + H]+ calcd for $C_{31}H_{42}NO_5^+$ 508.3057, found 508.3046; [M + Na]+ calcd for $C_{23}H_{33}NaO_4^+$ 530.2877, found 530.2869. IR (thin film, cm^{-1}): 3410, 2919, 2851, 1731, 1601, 1503, 1448, 1377, 1242, 1169, 1093, 1020, 893, 822, 748, 694, 613, 583, 569, 560, 551, 544, 529. $[a]_D^{23}$ = +12.9 (c = 0.1, CH_2Cl_2).

Acknowledgments

PN is grateful to NIH (R35 GM136341) for supporting these studies, and to NSF grant CHE-1955069 for supporting the synthesis of the CPA catalysts and Hantzsch esters used in this article. PN also thanks the National Cancer Institute Development Therapeutics Program (NCI/DTP) https://dtp.cancer.gov for providing screening data of compounds present in this manuscript (Specifically, NSC# of **8a**, **11a**, **11c**, and **13a–f** are 852083, 852085, 852084, 852077, 852082, 852081, 852078, 852079, and 852080). We also thank Prof. Nathaniel Szymczak for providing Ru(bpi)$(PPh_3)_2$Cl and Ru(^{Me}bpi)(PPh_3)Cl catalysts for these studies. In addition, we thank Prof. Matthew Soellner (University of Michigan) for the useful discussions during the preparation of this manuscript. GS gratefully acknowledges funding for this project from the CJD Foundation and an operating grant from the Canadian Institutes for Health Research (CIHR #202209PJT).

Conflict of Interest

The authors declare no conflict of interest.

Data Availability Statement

The data that support the findings of this study are available in the supplementary material of this article.

Keywords: analog · anticancer activity · cardiotonic steroid · chiral phosphoric acid · diastereoselective · reductive amination

© 2025 The Author(s). Chemistry – A European Journal published by Wiley-VCH GmbH

[1] W. Withering, *An Account of the Foxglove and Some of ist Medical Uses*, G.G.J. and Robinson, Birmingham **1785**.
[2] a) T. W. Smith, *N. Engl. J. Med.* **1973**, *288*, 719; b) T. W. Smith, *N. Engl. J. Med.* **1973**, *288*, 942.
[3] a) H. J. Schatzmann, *Helv. Physiol. Phamracol. Acta*. **1953**, *11*, 346; b) J. C. Skou, *Biochim. Biophys. Acta* **1957**, *23*, 394.
[4] a) T. Mijatovic, E. Van Quaquebeke, B. Delest, O. Debeir, F. Darro, R. Kiss, *Biochim. Biophys. Acta (BBA) – Rev. Cancer*, **2007**, *1776* 32; b) P. Babula, M. Masarik, V. Adam, I. Provaznik, R. Kizek, *Anti-Cancer Agents Med. Chem.* **2013**, *13*, 1069; c) N. F. Zanchett Scheider, C. Cerella, C. M. Oliveira Simões, M. Diederich, *Molecules* **2017**, *22*, 1932.
[5] a) M. Mehrabian, X. Wang, S. Eid, B. Q. Yan, M. Grinberg, M. Siegner, C. Sackmann, M. Sulman, W. Zhao, D. Williams, G. Schmitt-Ulms, *PLoS One* **2022**, *17*, e0270915; b) S. Eid, T. Zerbes, D. Williams, X. Wang, C. Sackmann, S. Meier, O. N. P. N. Dulin, G. Schmitt-Ulms, *Int. J. of Mol. Sci.* **2022**, *23*, 14823; c) S. Eid, W. Zhao, D. Williams, Z. Nasser, J. Griffin, P. Nagorny, G. Schmitt-Ulms, *PLoS One* **2024**, *19*, e0308821; d) A. A. Markina, R. B. Kazanskaya, J. A. Timoshina, V. A. Zavialov, D. A. Abaimov, A. B. Volnova, T. N. Fedorova, R. R. Gainetdinov, A. V. Lopachev, *Biomedicines* **2023**, *11*, 1820.
[6] a) Y.-H. Jin, S. Jeon, J. Lee, S. Kim, M. S. Jang, C. M. Park, J. H. Song, H. R. Kim, S. Kwon, *Pharmaceutics* **2021**, *13*, 1839; b) H. R. El-Seedi, N. Yosri, B. El-Aarag, S. H. Mahmoud, A. Zayed, M. Du, A. Saeed, S. G. Musharraf, I. M. El-Garawani, M. R. Habib, H. E. Tahir, M. M. Hegab, X. Zou, Z. Guo, T. Efferth, S. A. M. Khalifa, *Molecules* **2022**, *27*, 6586; c) K. S. Plante, V. Dwivedi, J. A. Plante, D. Fernandez, D. Mirchandani, N. Bopp, P. V. Aguilar, J.-G. Park, P. P. Tamayo, J. Delgado, V. Shivanna, J. B. Torrelles, L. Martinez-Sobrido, R. Matos, S. C. Weaver, K. J. Sastry, R. A. Newman, *Biomed. & Pharmacother.* **2021**, *138*, 111457.
[7] a) A. M. Orellana, P. F. Kinoshita, J. A. Leite, E. M. Kawamoto, C. Scavone, *Front. in Endocrin* **2016**, *7*, 10; b) J. A. Leite, L. H. A. Cavalcante-Silva, M. R. Ribeiro, G. de Morais Lima, C. Scavone, S. Rodrigues-Mascarenhas, *Front. in Pharmacol.* **2022**, *13*, 824907; c) R. Rutkoski, L. K. Debarba, L. Stilgenbauer, T. Rosenthal, M. Sadagurski, P. Nagorny, *ACS Med. Chem. Lett.* **2024**, *15*, 280; d) D. A. Ferreira, A. B. A. Medeiros, M. M. Soares, E. de Almeida Lima, G. C. S. L. de Oliveira, M. B. da Silva Leite, M. V. Machado, J. A. F. P. Villar, L. A. Barbosa, C. Scavone, M. T. Moura, S. Rodrigues-Mascarenhas, *Cells* **2024**, *13*, 1568; e) I. J. P. Garcia, P. F. Kinoshita, I. de Oliveira Braga, G. M. Parreira, J. A. Mignaco, C. Scavone, L. A. Barbosa, H. de Lima Santos, *J. of Cell. Biochem.* **2018**, *119*, 2156.
[8] a) H. Lee, D. Wilson, K. V. Bunting, D. Kotecha, T. Jackson, *Ageing Res. Rev.* **2023**, *86*, 101860; b) V. Smer-Barreto, A. Quintanilla, R. J. R. Elliott, J. C. Dawson, J. Sun, V. M. Campa, A. Lorente-Macias, A. Unciti-Broceta, N. O. Carragher, J. C. Acosta, D. A. Oyarzun, *Nat. Commun* **2023**, *14*, 3445; c) N. Martin, O. Soriani, D. Bernard, *Trends Mol. Med.* **2020**, *26*, 243; d) A. Guerrero, N. Herranz, B. Sun, V. Wagner, S. Gallage, R. Guiho, K. Wolter, J. Pombo, E. E. Irvine, A. J. Innes, J. Birch, J. Glegola, S. Manshaei, D. Heide, G. Dharmalingam, J. Harbig, A. Olona, J. Behmoaras, D. Dauch, A. G. Uren, L. Zender, S. Vernia, J. P. Martinez-Barbera, M. Heikenwalder, D. J. Withers, *Nat. Metab.* **2019**, *11*, 1074.
[9] a) G. Gurkan, M. A. Erdogan, G. Karahan, H. Kaya, G. Yigitturk, C. Kizmazoglu, O. Erbas, *Turk. Neurosurg.* **2023**, *33*, 258; b) H. E. Titus, H. Xu, A. P. Robinson, P. A. Patel, Y. Chen, D. Fantini, V. Eaton, M. Karl, E. D. Garrison, I. V. L. Rose, M. Y. Chiang, J. R. Podojil, R. Balabanov, S. A. Liddelow, R. H. Miller, B. Popko, S. D. Miller, *Glia* **2022**, *70*, 1950; c) E. V. Lopatina, I. L. Yachnev, V. A. Penniyaynen, V. B. Plakhova, S. A. Podzorova, T. N. Shelykh, I. V. Rogachevsky, I. P. Butkevich, V. A. Mikhailenko, A. V. Kipenko, B. V. Krylov, *Med. Chem.* **2012**, *8*, 33.
[10] a) M. Luta, A. Hensel, W. Kreis, *Steroids* **1998**, *63*, 44; b) H. Jin, T. Y. R. Tsai, K. Wiesner, *Can. J. Chem.* **1983**, *61*, 2442; c) J. M. Langenhan, N. R. Peters, I. A. Guzei, M. Hoffmann, J. S. Thorson, *Proc. Nat. Acad. Sci. U.S.A* **2005**, *102*, 12305; d) M. Zhou, G. A. O'Doherty, *Org. Lett.* **2006**, *8*, 4339; e) A. K. V. Iyer, M. Zhou, N. Azad, H. Elbaz, L. Wang, D. K. Rogalsky, Y. Rojanasakul, G. A. O'Doherty, J. M. Langenhan, *ACS Med. Chem. Lett.* **2010**, *1*, 326; f) Y. Ma, Z. Li, H. Shi, J. Zhang, B. Yu, *J. Org. Chem.* **2011**, *76*, 9748; g) H.-Y. L. Wang, W. Xin, M. Zhou, T. A. Stueckle, Y. Rojanaskul, G. A. O'Doherty, *ACS Med. Chem. Lett.* **2011**, *2*, 73; h) H.-Y. L. Wang, B. Wu, Q. Zhang, S.-W. Kang, Y. Rojanasakul, G. A. O'Doherty, *ACS Med. Chem. Lett.* **2011**, *2*, 259; i) H.-Y. L. Wang, Y. Rojanasakul, G. A. O'Doherty, *ACS Med. Chem. Lett.* **2011**, *2*, 264; j) J. M. Langenhan, M. M. Endo, J. M. Engle, L. L. Fukumoto, D. R. Rogalsky, L. K. Slevin, L. R. Fay, R. W. Lucker, J. R. Rohlfing, K. R. Smith, A. E. Tjaden, H. M. Werner, *Carbohydr. Res.* **2011**, *346*, 2663; k) J. W. Hinds, S. B. McKenna, E. U. Sharif, H.-Y. L. Wang, N. G. Akhmedov, *ChemMedChem* **2013**, *8*, 63; l) K. N. Baryal, S. Adhikari, J. Zhu, *J. Org. Chem.* **2013**, *78*, 12469; m) J. Zhang, L. V. Ponomareva, N. S. Nandurkar, Y. Yuan, L. Fang, C.-G. Zhan, J. S. Thorson, *ACS Med. Chem. Lett.* **2015**, *6*, 1053; n) D. Ainembabazi, X. Geng, N. S. Gavande, J. J. Turchi, Y. Zhang, *ChemMedChem* **2022**, *17*, e202200415.
[11] H. R. Khatri, B. Bhattarai, W. Kaplan, Z. Li, M. J. C. Long, Y. Aye, P. Nagorny, *J. Am. Chem. Soc.* **2019**, *141*, 4849.
[12] J.-H. Tay, V. Dorokhov, S. Wang, P. Nagorny, *J. Antibiot. (Tokyo)* **2019**, *72*, 437.
[13] B. Liu, S. Bi, J. Wang, P. Xu, B. Yu, *Org. Lett.* **2024**, *26*, 8725.
[14] X. Li, Y. Ren, Y. Bao, J. Liu, X. Zhang, Y. Zhang, X.-L. Sun, X. Yao, J.-S. Tang, *Eur. J. Med. Chem.* **2018**, *145*, 252.
[15] a) H. M. A. M. Qazzaz, S. L. Goudy, R. Valdes, *J. Biol. Chem.* **1996**, *271*, 8731; b) D. Ni, T. L. Madden, M. Johansen, E. Felix, D. H. Ho, R. A. Newman, *J. Exp. Therap. & Oncol.* **2002**, *2*, 278.
[16] a) L. Boff, L. Persich, P. Brambila, F. M. Ottoni, J. Munkert, G. S. Ramos, A. R. S. Viana, W. Kreis, F. C. Braga, R. J. Alves, R. M. de Padua, N. F. Z. Schneider, C. M. O. Simoes, *Anti-Cancer Drugs* **2020**, *31*, 452; b) R. M. de Padua, J. M. Kratz, J. Munkert, J. W. Bertol, C. Rigotto, D. Schuster, V. G. Maltarollo, W. Kreis, C. M. O. Simoes, F. C. Braga, *Chem. Biodiversity* **2022**, *19*, e202200411.
[17] a) M. Adamczyk, J. Grote, *Steroids* **1996**, *61*, 562; b) M. Adamczyk, J. Grote, *Biorg. & Med. Chem. Lett.* **1999**, *9*, 771.
[18] a) E. Hauser, U. Boffo, L. Meister, L. Sawlewicz, H. H. A. Linde, K. Meyer, *Helv. Chim. Acta* **1973**, *56*, 286; b) D. C. Humber, P. S. Jones, G. H. Phillipps, *Steroids* **1983**, *42*, 3154.
[19] a) J. Lee, A. Borovika, Y. Khomutnyk, P. Nagorny, *Chem. Commun.* **2017**, *53*, 8976; b) J.-H. Tay, A. J. Arguelles, M. D. DeMars II, P. M. Zimmerman, D. H. Sherman, P. Nagorny, *J. Am. Chem. Soc.* **2017**, *139*, 8570; c) S. Wang, A. J. Arguelles, J.-H. Tay, M. Hotta, P. M. Zimmerman, P. Nagorny, *Chem. Eur. J.* **2020**, *26*, 4583.
[20] a) C. Tichvon, E. Zviagin, Z. Surma, P. Nagorny, *Org. Lett.* **2024**, *26*, 2445; b) N. Carney, N. Perry, J. Garabedian, P. Nagorny, *Org. Lett.* **2023**, *6*, 966; c) Z. Fejedelem, N. Carney, P. Nagorny, *J. Org. Chem.* **2021**, *86*, 10249; d) B. Bhattarai, P. Nagorny, *Org. Lett.* **2018**, *20*, 154; e) W. Kaplan, H. R. Khatri, P. Nagorny, *J. Am. Chem. Soc.* **2016**, *138*, 7194.
[21] a) E. W. Baxter, A. B. Reitz, *Org. React.* **2002**, *59*, 1785; b) O. I. Afanasyev, E. Kuchuk, D. L. Usanov, D. Chusov, *Chem. Rev.* **2019**, *119*, 11857.
[22] a) For selected reviews of CPA-catalyzed transfer hydrogenations refer to: D. Parmar, E. Sugiono, S. Raja, M. Rueping, *Chem. Rev.* **2014**, *114*, 9047; b) S. Das, V. N. Wakchaure, B. List, *Organocatalytic Asymmetric Transfer Hydrogenation Reactions. Asymmetric Hydrogenation and Transfer Hydrogenation, First Edition*, V. Ratovelomanana-Vidal, P. Phansavath, (Ed.), WILEY-VCH GmbH, **2021**, p. 339; c) A. M. Palvolgyi, F. Scharinger, M. Schnurch, K. Bica-Schroder, *Eur. J. Org. Chem.* **2021**, *38*, 5367.
[23] S. Singh, U. K. Batra, *Indian J. Chem. Sect. B.* **1989**, *28*, 1.
[24] a) S. Hoffmann, A. M. Seayad, B. List, *Angew. Chem. Int. Ed.* **2005**, *44*, 7424; b) M. Rueping, E. Sugiono, C. Azap, T. Theissmann, M. Bolte, *Org. Lett.* **2005**, *7*, 3781; c) R. I. Storer, D. E. Carrera, Y. Ni, D. W. C. MacMillan, *J. Am. Chem. Soc.* **2006**, *128*, 84.
[25] a) For the selected examples of using chiral catalysis to accomplish diastereoselective reduction of natural products refer to: E. R. Welin, A. Ngamnithiporn, M. Klatte, G. Lapointe, G. M. Pototschnig, M. S. J. McDermott, D. Conklin, C. D. Gilmore, P. M. Tadross, C. K. Haley, K. Negoro, E. Glibstrup, C. U. Grunanger, K. M. Allan, S. C. Virgil, D. J. Slamon, B. M. Stoltz, *Science* **2019**, *363*, 270; b) D. N. Le, E. Hansen, H. A. Khan, B. Kim, O. Wiest, V. M. Dong, *Nat. Chem* **2018**, *10*, 968; c) Y. Chen, Y.-M. He, S. Zhang, T. Miao, Q.-H. Fan, *Angew. Chem. Int. Ed.* **2018**, *58*, 3809; d) S. D. Stone, N. J. Lajkiewicz, L. Whitesell, A. Hilmy, J. A. Porco, Jr., *J. Am. Chem. Soc.* **2015**, *137*, 525; e) F. Balssa, M. Fischer, Y. Bonnaire, *Steroids* **2014**, *86*, 1; f) D. B. Ramachary, R. Sakthidevi, P. S. Reddy, *RSC Adv.* **2013**, *3*, 13497; g) S. Bell, B. Wustenberg, S. Kaiser, F. Menges, T. Netscher, A. Pfaltz, *Science* **2006**, *311*, 642; h) C. Chen, M. E. Layton, S. M. Sheehan, M. D. Shair, *J. Am. Chem. Soc.* **2000**, *122*, 7424; i) M. Kurosu, Y. Kishi, *J. Org. Chem.* **1998**, *63*, 6100; j) J.-C. Poulin, H. B. Kagan, *J. Chem. Soc. Chem. Commun.* **1982**, 1261.
[26] For a related CPA-catalyzed reductive amination of tetralones refer to: D. Y. Park, K.-H. Kim, C.-H. Cheon, *Adv. Synth. Catal.* **2018**, *360*, 462.
[27] C. Zhu, T. Akiyama, *Org. Lett.* **2009**, *11*, 4180.

© 2025 The Author(s). Chemistry – A European Journal published by Wiley-VCH GmbH

[28] a) R. A. Newman, K. J. Sastry, R. Avrav-Boger, H. Cai, R. Matos, R. Harrod, *J. Exp. Phamocol.* **2020**, *12*, 503; b) T. Mekhail, H. Kaur, R. Gnapathi, T. G. Budd, P. Elson, R. M. Bukowski, *Invest. New Drugs.* **2006**, *24*, 423; c) M. T. Roth, D. B. Cardin, E. H. Borazanci, M. Steinbach, V. J. Picozzi, A. Rosemury, R. C. Wadlow, R. A. Newman, J. Berlin, *Oncologist.* **2020**, *25*, e1446.
[29] K. Michalak, L. Rarova, M. Kubala, T. Stenclova, M. Strnad, J. Wicha, *Eur. J. Med. Chem.* **2020**, *202*, 112520.
[30] S. S. Kim, K. Nehru, *Synlett* **2002**, *4*, 0616.
[31] S. S. Welankiwar; W. S. Murphy, *J. Chem. Soc., Perkin Trans.* **1976**, *1*, 710.
[32] K. S. Kim, I. H. Cho, B. K. Yoo, Y. H. Song, C. S. Hahn, *J. Chem. Soc. Chem. Commun.* **1984**, 762.
[33] R. Kavembu, P. Prabhakaran, K. Natarajan, *Coord. Chem. Rev.* **2005**, *249*, 911.
[34] a) K. T. Tseng, J. W. Kempf, N. K. Szymczak, *Organometallics* **2013**, *32*, 2046; b) K.-N. T. Tseng, J. W. Kampf, N. K. Szymczak, *ACS Catal.* **2015**, *5*, 5468.
[35] C. K. Hill, J. F. Hartwig, *Nat. Chem* **2017**, *9*, 1213.
[36] J. Li, S. Grosslight, S. J. Miller, M. S. Sigman, D. F. Toste, *ACS Catal.* **2019**, *9*, 9794.
[37] For selected examples of such studies refer to: a) L. Simon, J. M. Goodman, *J. Am. Chem. Soc.* **2008**, *130*, 8741; b) A. Shoja, J. P. Reid, *J. Am. Chem. Soc.* **2021**, *143*, 7209; c) J. Gramuller, M. Franta, R. M. Gschwind, *J. Am. Chem. Soc.* **2022**, *144*, 19861; d) M. Franta, A. Pattanaik, W. Silva, K. Motiram-Corral, J. Rehbein, R. M. Gschwind, *J. Am. Chem. Soc.* **2025**, *147*, 2549;
[38] The results of 5-dose NCI-60 evaluation of digitoxigenin (NSC# 407806) and digitoxin (NSC# 7529) were obtained from the National Cancer Institute website (www.dtp.cancer.gov).
[39] W. Zhao, S. Eid, C. Sackmann, D. Williams, X. Wang, Y. Ouyang, T. Zerbes, G. Schmitt-Ullms, *bioRxiv* **2024**, https://doi.org/10.1101/2024.12.18.629254
[40] J. Zhao, J. Bai, X. Yu, W. Zhang, C. Zhao, J. Ye, P. Wei, K. He, J. Zou, *Mol. Diversity* **2025**, *29*, 2617.

Manuscript received: April 25, 2025
Revised manuscript received: June 12, 2025
Version of record online: June 27, 2025

© 2025 The Author(s). Chemistry – A European Journal published by Wiley-VCH GmbH